Sarang Thombre

**Test Bench Solutions for Advanced GNSS Receivers:
Implementation, Automation, and Application**

Tampere 2014

Sarang Thombre

Test Bench Solutions for Advanced GNSS Receivers: Implementation, Automation, and Application

Thesis for the degree of Doctor of Science in Technology to be presented with due permission for public examination and criticism in Tietotalo Building, Auditorium TB224, at Tampere University of Technology, on the 4th of April 2014, at 12 noon.

Supervisors:

Jari Nurmi, Dr. Tech., Professor
Department of Electronics and Communications Engineering,
Tampere University of Technology,
Tampere, Finland.

Mikko Valkama, Dr. Tech., Professor
Department of Electronics and Communications Engineering,
Tampere University of Technology,
Tampere, Finland.

Pre-examiners:

Gérard Lachapelle, Dr.Tech., Professor

Professor and CRC/iCORE Chair in Wireless Location.
University of Calgary, Department of Geomatics Engineering,
2500 University Dr NW
Calgary, Alberta, Canada T2N 1N4.

Marco Lisi, Dottore ingegnere.

GNSS Services Engineering Manager,
Special Advisor of the European Commission.
European Space Research & Technology Centre (ESTEC),
Keplerlaan 1, 2201 AZ Noordwijk, The Netherlands.

Opponents:

Marco Lisi, Dottore ingegnere.

GNSS Services Engineering Manager,
Special Advisor of the European Commission.
European Space Research & Technology Centre (ESTEC),
Keplerlaan 1, 2201 AZ Noordwijk, The Netherlands.

Jari Syrjärinne, D.Sc.(Tech)

HERE, a Nokia business
PL 14, 33721 TAMPERE
Finland.

ABSTRACT

Considerable study has been devoted to the implementation of GNSS receivers for diverse applications, and to finding solutions to some of the non-idealities associated with such receivers. However, not much research is devoted to innovations in their performance evaluation, even though this is an integral step in the overall implementation process. This research work attempts to address this issue through three different perspectives: by focusing on innovation in the testing procedures and test-bench implementation, its automation and its application to advanced multi-frequency, multi-constellation GPS and Galileo receivers. Majority of this research was conducted within the GREAT, GRAMMAR, and FUGAT projects funded by EU FP6/FP7 and TEKES respectively, during which the author was responsible for designing test-scenarios and performing validations of the implemented receiver solution.

The first part of the research is devoted to the study and design of sources of test signals for an advanced GNSS receiver test-bench. An in-depth background literature study was conducted on software-based GNSS signal simulators to trace their evolution over the past two decades. Keeping their special features and limitations in view, recommendations have been made on the optimum architecture and essential features within such simulators for testing of advanced receivers. This resulted in the implementation of an experimental software-based simulator capable of producing GPS L1 and Galileo E1 signals at intermediate frequency. Another solution investigated was a GNSS Sampled Data Generator (SDG) based on wideband sampling. This included designing the entire radio front-end operating on the bandpass-sampling principle. The low noise amplifier designed as part of this SDG has been implemented on a printed circuit board.

Phase noise (PN) from the radio front-end's local frequency generator (LFG) is a source of error that has hitherto not been included in any GNSS signal simulator. Furthermore, the characterization of the baseband tracking loops in presence of this phase noise has not yet been included in the typical receiver test scenarios. The second part of this research attempts to create mathematical models representing the LFG's phase noise contribution,

first for a free running oscillator and later for a complete phase-locked loop (PLL). The effect of such phase noise was studied on the baseband correlation performance of GPS and Galileo receivers. The results helped to demonstrate a direct relation between the PN and the baseband tracking performance, thus helping to define guidelines for radio front-end PLL circuit design in order to maintain a minimum baseband tracking performance within the GNSS receiver.

The final part of this research work focusses on describing the automated test-bench developed at Tampere University of Technology (TUT) for analyzing the overall performance of multi-frequency multi-constellation GNSS receivers. The proposed test-bench includes a data capture tool to extract internal process information, and the overall controlling software, called automated performance evaluation tool, that is able to communicate between all modules for hands-free, one-button-click testing of GNSS receivers. Furthermore, these tools have been applied for the single frequency GPS L1 performance testing of the TUTGNSS receiver, with recommendations on how they can be adapted to testing of advanced multi-frequency, multi-constellation receivers.

PREFACE

The work presented in this thesis has been carried out under the supervision of Prof. Jari Nurmi and Prof. Mikko Valkama during the years 2010 - 2013 within the Department of Computer Systems and its successor, the Department of Electronics and Communications Engineering of the Tampere University of Technology, Finland.

I am grateful towards Prof. Nurmi for allowing me the research freedom during the past years to investigate a topic which is quite ubiquitous within the industrial domain, yet not fully explored within academic circles. He has been very supportive and encouraging, offering me new vistas for applying skills that I have attempted to gather over the past few years. It has been a real pleasure for me to be a part of his research group. I would also like to appreciate the technical advice and supervision provided to me by Prof. Mikko Valkama, who is most appropriate to verify whether a particular research idea possesses sound technological feasibility. Prof. Gérard Lachapelle and Dr. Marco Lisi have been the external reviewers for this manuscript, and I would like to acknowledge them for their valuable feedback and suggestions on improvements. Finally, I would like to thank Dr. Jari Syrjärinne and Dr. Marco Lisi for agreeing to be the opponents at my Doctoral dissertation, and through it providing me with constructive criticism while I defended my research work.

In addition to my direct supervisors, other experts who have guided me during the formative years of my Doctoral research career are Dr. Heikki Hurskainen, Associate Prof. Elena Simona Lohan, Dr. Stephan Sand, Dr. Nikolay N. Tchamov, Ernesto Perez Serna, Marco Detratti, Dr. L. Enrique Aguado, Ignacio Fernández Hernández, Ari Asp, Dr. Tiiti Kellomäki, Dr. Martti Kirkko-Jaakkola and Prof. John Raquet. I would like to sincerely thank them for their valuable and timely insights into matters of technology.

Tampere, 4th April, 2014
Sarang Thombre

TABLE OF CONTENTS

LIST OF PUBLICATIONS

This thesis is a compilation of the following publications, referred to as [P#] and are appended in the concluding half of the thesis.

[P1]   **S. Thombre**, E. S. Lohan, J. Raquet, H. Hurskainen, J. Nurmi, "Software-based GNSS Signal Simulators: Past, Present and Possible Future", Proceedings of the *2010 European Navigation Conference (ENC GNSS 2010)*, October 2010 in Braunschweig, Germany.

[P2]   **S. Thombre**, H. Hurskainen, J. Nurmi, "Wideband, High Gain, High Linearity, Low Noise Amplifier for GNSS Frequencies with Compensation for Low Frequency Instability", Proceedings of the *Advanced Satellite Multimedia Systems Conference (ASMS 2010)*, September 2010 in Cagliari, Italy.

[P3]   **S. Thombre**, J. Nurmi, "Bandpass-Sampling based GNSS Sampled Data Generator – A Design Perspective", Proceedings of the *International Conference on Localization and GNSS (ICL-GNSS 2012)*, June 2012 in Starnberg, Germany.

[P4]   E. P. Serna, **S. Thombre**, M. Valkama, S. Lohan, V. Syrjälä, M. Detratti, H. Hurskainen, J. Nurmi, "Local Oscillator Phase Noise Effects on GNSS Code Tracking", *InsideGNSS*, Nov/Dec 2010, pg 52-62.

[P5]   **S. Thombre**, J. Raasakka, M. Valkama, S. Lohan, H. Hurskainen, J. Nurmi, "Local Oscillator Phase Noise Effects on Phase Angle Component of GNSS Code Correlation", Proceedings of the *2011 International Conference on Localization and GNSS (ICL-GNSS 2011)*, June 2011 in Tampere, Finland.

[P6]   **S. Thombre**, N. N. Tchamov, S. Lohan, M. Valkama, J. Nurmi, "Effects of Radio Front-end PLL Phase Noise on GNSS Baseband Correlation", accepted for publication in *NAVIGATION, Journal of the Institute of Navigation*, 21st March, 2014.

[P7]   **S. Thombre**, J. Raasakka, T. Paakki, F. Della Rosa, M. Valkama, J. Nurmi, "Automated Test-bench Infrastructure for GNSS Receivers – Case Study of the

TUTGNSS Receiver", Proceedings of the *Institute of Navigation's GNSS+ (ION GNSS+ 2013)*, Nashville, Tennessee, USA, September 16-20, 2013.

LIST OF ABBREVIATIONS

2D	Two-dimensional
3D	Three-dimensional
ADC	Analog-to-Digital Converter
AutoPET	Automated Performance Evaluation Tool
AV	Allan Variance
AWGN	Additive White Gaussian Noise
BW	Bandwidth
BPF	Bandpass Filter
C/A	Coarse Acquisition
CHPLL	Charge Pump PLL
CNR	Carrier to Noise Ratio
DC	Direct Current
dCAP	Data Capture Tool
DLR	German Aerospace Center
ENC	European Navigation Conference
ELT	Department of Electronics and Communications Engineering
ESA	European Space Agency
EU FP	European Union Framework Programme
FDR	Frequency Division Ratio
FLL	Frequency Locked Loop
FPGA	Field Programmable Gate Array
FRO	Free Running Oscillator
FUGAT	Future GNSS Applications and Techniques
GALILEO	European Satellite Navigation System
GLONASS	Globalnaya Navigatsionnaya Sputnikovaya Sistema
GNSS	Global Navigation Satellite System
GPS	Global Positioning System
GRAMMAR	Galileo Ready Advanced Mass Market Receiver
GREAT	Galileo Receiver for Mass Market

HI	Human Interface
HSSP	High Speed Signal Processing unit
HW	Hardware
ICD	Interface Control Document
IEEE	Institute of Electrical and Electronics Engineers
IC	Integrated Circuit
IF	Intermediate Frequency
ION	Institute of Navigation
IRNSS	Indian Regional Navigation Satellite System
LC	Local Control unit
LFG	Local Frequency Generator
LNA	Low Noise Amplifier (Ampl.)
LPF	Low Pass Filter
LSSP	Low Speed Signal Processing Unit
LO	Local Oscillator
PFD	Phase and Frequency Detector
PIT	Pre-detection Integration Time
PLL	Phase locked Loop
PN	Phase Noise
PRN	Pseudo Random Noise
PS	Protocol Stack
PSD	Power Spectral Density
PVT	Position Velocity Time
QZSS	Japanese Quasi-zenith Satellite System
RF FE	Radio Frequency Front-end
RO	Reference Oscillator
RS-232	Recommended Standard – 232 (serial port)
RUT	Receiver Under Test
SDG	Sampled Data Generator
SDR	Software Defined Radio
SNR	Signal-to-Noise Ratio
SW	Software

TEKES	Finnish Funding Agency for Technology and Innovation
TTFF	Time to First Fix
TUT	Tampere University of Technology
TUTGNSS	TUT's Prototype GNSS Receiver
TUTGSSS	TUT's Prototype GNSS Signal Simulator in Software
USB	Universal Serial Bus
VCO	Voltage Controlled Oscillator
VHDL	Very High Speed Integrated Circuit Hardware Description Language

LIST OF SYMBOLS

ρ_s	Pseudorange between one satellite and the user
(x_s, y_s, z_s)	Coordinates of satellite position
(x_u, y_u, z_u)	Coordinates of user position
c	Speed of light
t_u	Time offset between satellite system and the user receiver clocks
$I_{carrier}$	In-phase component of the carrier signal
$Q_{carrier}$	Quadrature-phase component of the carrier signal
A	Signal Amplitude
$f_{carrier}$	Carrier frequency
$t_{carrier}$	Time parameter of the carrier signal
t_{code}	Time parameter of code signal
$AV(\tau)$	Allan Variance computed over time τ
M	Number of samples over which Allan Variance is computed
$y(\tau)_i$	Value of ith sample
dt	Satellite clock error
a_0	Satellite clock time offset in seconds
a_1	Fractional satellite clock frequency offset
a_2	Fractional satellite clock frequency drift
t	Time
t_{oc}	Reference epoch in seconds
$n(h)$	Electron density at height h
n_{max}	Peak electron density
h_{max}	Height of peak electron density
B	Thickness of the ionospheric layer
$dTropo^{MH}$	Tropospheric delay using the Modified Hopfield model
$dTropo^{GG}$	Slant tropospheric delay with the Goad & Goodman model
$P(t)$	Time variant pressure parameter
$T(t)$	Time variant temperature parameter

$H(t)$	Time variant humidity parameter
$El(t)$	Elevation angle
w	Gaussian white noise
T_r^S	Tropospheric error in meters
N	Refractive index along the signal path
a	Upper limit of tropospheric boundary in meters
b	Lower limit of tropospheric boundary in meters
$r_{E1}(t)$	Galileo E1 received signal after the transmission channel
α_i	Complex path coefficient for path i
τ_i	Path delay for path i
n	Additive white Gaussian noise
f_{ci}	Center frequency of band i
f_{smin}	Minimum sampling frequency
f_{IFi}	Intermediate frequency of band i
f_s	Sampling frequency
BWi	Bandwidth of band i
$Rem\left(\frac{X}{Y}\right)$	Remainder after dividing X with Y
$Int[x]$	Largest integer smaller than or equal to x
n_i	Signal spectrum segment number
f_{Hi}	Higher frequency limit of the signal band
f_{Li}	Lower frequency limit of the signal band
m	Replica number of the sampled band
N_{Phase}	Phase noise
K	Boltzmann constant
T	Temperature in Kelvin
P_{Signal}	Power of the signal under consideration (in absolute values)
ω_0	Center frequency of the signal under consideration in radians/sec
Q	Quality factor of the resonator in the local oscillator
$\Delta\omega$	Frequency offset from center frequency at which PN is computed
$\emptyset$	Phase noise

LIST OF FIGURES

LIST OF TABLES

1. INTRODUCTION

1.1   Background and Motivation

Global Navigation Satellite Systems (GNSS) include the American NAVSTAR Global Positioning System (GPS), European GALILEO, Russian GLONASS, and the Chinese BeiDou-2/COMPASS system. Satellite navigation systems that are planned to be regional in their geographic scope include the Indian Regional Navigation Satellite System (IRNSS), and Japanese Quasi-zenith Satellite System (QZSS). The architecture of each of these systems is similar, consisting of three segments – Space, Ground, and User [29], [30], [31]. The Space Segment consists of a constellation of satellites which transmit the radio-navigation signals towards the Earth, the Ground Segment consists of a network of ground-based monitoring, control, tracking and uplink stations, and the User Segment consists of the receivers that provide the position, velocity, time (PVT) and navigation solutions.

Receiver design and innovation has attracted considerable attention and effort from the GNSS research community. This also includes research in overcoming limitations of power, size, speed, and cost, finding solutions to errors introduced due to atmospheric composition and multipath, and innovations in multi-frequency, multi-constellation receiver design. However, in-depth discussions, studies, and debates on the testing and performance evaluation of GNSS receivers are sorely missing from industrial and academic discourses. This has resulted in a considerable growth in the diversity of testing procedures, and yet the number of receiver parameters to be tested or innovation in the methodology of performing these testing procedures has remained limited and even

primitive in some cases. It has been noticed from a background literature review that very few research manuscripts are dedicated to innovations in testing and performance evaluation of GNSS receivers.

The prototype Global Navigation Satellite System receiver (TUTGNSS) [1], developed at the Department of Electronics and Communications Engineering (ELT) of Tampere University of Technology, is now in the performance testing phase. TUTGNSS is a GPS L1/L5 + Galileo E1/E5a dual-frequency dual-constellation receiver, jointly developed by TUT and its international partners under two European Union and a TEKES research grant. These included the Galileo Ready Advanced Mass Market Receiver (GRAMMAR), Galileo Receiver for Mass Market (GREAT), and Future GNSS Applications and Techniques (FUGAT) projects, aimed at a highly innovative approach to developing a prototype consumer–grade dual-frequency dual-constellation GNSS receiver, targeted at mass market applications with the widest potential exploitation (this is also the definition of 'advanced' GNSS receivers that is henceforth targeted in this manuscript).

With the advent of such advanced GNSS receivers capable of multi-frequency, multi-constellation operations, it is no longer sufficient to continue using the testing procedures and the related test-bench infrastructure that was used until now for 'simple' single frequency single constellation receivers.

Therefore, it was during the implementation of these projects that the author had the opportunity to conduct research on advanced GNSS receiver technology and contribute towards the creation of an innovative test plan, design the corresponding test scenarios and test facility, execute receiver testing, document test results and the user manual, troubleshoot the dual-frequency, dual-constellation prototype receiver, and facilitate the approval of the project from the external reviewers. This thesis manuscript is an accumulation of the experiences and scientific publications emanating from working on these projects, technologies and ideas during the past four years.

1.2   *Research Objectives and Scope*

Three major questions related to test-bench solutions for advanced GNSS receivers were addressed during the progress of this research:

- Is it possible to design innovative sources of test signals?
- Is it possible to locate new test parameters within the receiver that could offer new view-points for determining its performance?
- Is it possible to automate the entire testing process to improve reliability, accuracy and efficiency?

Therefore, the primary objective of this research work was to investigate novel techniques for performance evaluation of GNSS receivers. Building on this objective, the research scope included investigating innovative sources of test signals, inclusion of new parameters to test, adapting the test-cases and procedures for multi-frequency, multi-constellation receivers, and introducing automation and open-box testing (where it is possible to access the signal-flow within the system) into the overall test-plan. As mentioned in Section 1.1, the TUTGNSS receiver is capable of GPS L1/L5 + Galileo E1/E5a operation and consequently, this combination of frequencies and constellations sets the scope of the research work. Some of the research results are presented for the GPS L1 mode due to limitations of test-infrastructure within the research group.

The scope of the research was also bounded by the limitations of time, and the need for investigating multiple leads in an effort to diversify the research area. As an example, the radio front-end is the source of a number of RF non-linearities. However, here the scope is limited to the study of how the phase noise from its local frequency generator affects the receiver performance. It would be interesting for the future to investigate, e.g., the effect of differential group delay on the position accuracy of a multi-frequency receiver.

1.3   Linking the Thesis Topic to the Chapters and Publications

A block-diagram schematic of a typical GNSS receiver test-bench is shown in Fig. 1.1 Block 1 represents the source of test signals for Block 2, which denotes the receiver-under-test (RUT). Block 3 represents some intelligence, either human or machine, which
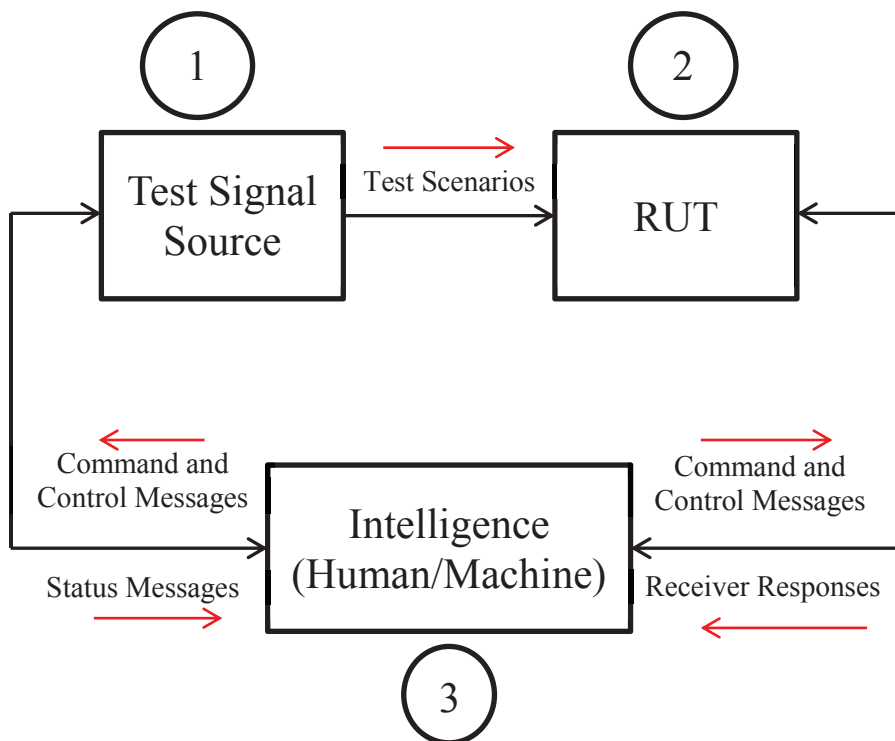
Fig. 1.1 Block Diagram of a typical GNSS receiver test-bench

Table 1.1 Linking the Thesis topic to the chapters and publications

Block	Chapters	Publications
Block 1	3, 4	[P1], [P2], [P3]
Block 2	5	[P4], [P5], [P6]
Block 3	6	[P7]

controls the entire testing process. It provides the test-scenarios and individual test-commands to Block 1, and simultaneously receives the responses from Block 2. In case of GNSS receivers, the communication between Blocks 1 and 2 and Block 3 can be full-duplex. This thesis work deals with innovation within each of these three Blocks. The Chapters within this manuscript are dedicated to describing the basic theory about these Blocks, while the novel research is then presented within the attached Publications [P1] – [P7]. The relation between the Publications, Thesis Chapters and the Block that each refers to is shown in Table 1.1

1.4 Research Methodology

This research utilized mostly a practical implementation methodology to reach the stated objectives and results. The research topic focusses more on innovations in the peripheral technologies associated with a GNSS receiver such as, source of test signals, test procedures, and test automation, rather than core signal processing tasks such as, acquisition, tracking and PVT computation. As can be deduced, the scope for innovation is more towards how these peripheral processes can be implemented with better efficiency and accuracy, and how they can be adapted for advanced receivers. This required working with software tools such as Matlab, Simulink, C language, VHDL, Agilent ADS, Qt, etc. and practically implementing the solutions. The need for creating breakthrough knowledge in the theoretical domain was out of scope of the research problem. However, the thesis does create new theoretical knowledge about the effect of phase noise on signal tracking, as this was necessary to demonstrate the need for proposing new parameters for more complete receiver characterization.

Another aspect of the methodology has been the focus on research collaboration. Due to the wide scope and inter-disciplinarity of the research topic, it was necessary to perform work-breakdown and delegate within the research group individual tasks related to the receiver design, development and performance evaluation. Furthermore, in situations where expert advice was necessary, as in the case of Simulink-based GNSS simulator implementation, and phase noise studies, collaborations with external research groups was

emphasized. The benefit has been a thorough peer-review of all the work performed and of every publication, and inclusion of best practices due to diversity of ideas. It should be noted however, that the bulk of the research work was performed by this researcher, as described in more detail in Chapter 7.

1.5   Main Contributions

This research has addressed the problem of innovations in GNSS receiver performance validation through three different perspectives - innovations in implementation of a test-bench, its automation techniques and application methodologies. The following are the main contributions and outcomes from this thesis work:

1. It presents an in-depth study of the state-of-art in software-based simulators for GNSS signals, including their evolution through three distinct generations [P1].

2. It describes essential modules and components of such simulators for testing advanced GNSS receivers, and proposes some mathematical models for their implementation [P1].

3. Based on this study, a GNSS signal simulator in software, called TUTGSSS and capable of producing GPS L1 and Galileo E1 B/C signals was implemented [P1].

4. The thesis describes an alternate solution for generating test-signals for performance testing of advanced GNSS receivers: a bandpass-sampling based sampled data generator, which is essentially a radio front-end capable of processing multiple GNSS frequencies [P2], [P3].

5. Implementation of the LNA within this radio front-end is described. The design, simulation, implementation and test results prove that the LNA successfully satisfied requirements of wide bandwidth, high gain, high linearity, frequency stability and low noise figure, and compares very well with the state-of-art in such amplifiers [P2].

6. The design and simulation of the filter stage and frequency planning for the bandpass-sampling analog-to-digital converter (ADC) of the radio frequency front-end (RF FE) is presented next. Optimum sampling frequency was computed to be

538.5 MHz and the resulting digital intermediate frequencies were 28.25 MHz and 155 MHz [P3].

7. This thesis presents an analytical approach to the evaluation of the effects of the RF FE's local frequency generator phase noise on the baseband tracking performance of a GNSS receiver, both in terms of a free running oscillator (FRO) and a PLL [P4], [P5], [P6].

8. The relation between integration time, PLL parameters and phase noise has been shown, and a criterion for radio front-end design has been presented [P4], [P5], [P6].

9. During this study a PLL phase noise model for GNSS applications was implemented which included PN contributions from each of its constituent building blocks [P6].

10. It includes a study on state-of-art in multi-frequency, multi-system GNSS receiver performance testing scenarios [P7].

11. An Automated Performance Evaluation Tool (AutoPET) was implemented for automated testing of GNSS receivers [P7].

12. A Data Capture Tool (dCAP) was implemented to access the signals at every stage of signal processing from inside the receiver hardware to identify the origin of signal anomalies [P7].

13. This thesis demonstrates the results of the GPS L1 performance evaluation of the TUTGNSS prototype receiver using the AutoPET and dCAP. Recommendations are made on how this testing can be enhanced to cover more advanced dual-frequency dual-constellation operating modes of the receiver [P7].

1.6   Thesis Outline

Because the thesis focus is on three different modules within the overall test-bench, the Chapters may at first glance appear as disjointed or unrelated to each other. It is hoped that Fig. 1.1 and Table 1.1, which describe how the individual Chapters within this thesis manuscript contribute to the overall research theme, will help the reader to view each Chapter as part of the whole.

Chapter 2 introduces the fundamental theory of satellite-based global navigation systems, including an introduction to the different receiver architectures. **Chapter 3** describes the software-based GNSS signal simulators. This includes a description of the various modules and components that constitute a typical software-based simulator. **Chapter 4** presents the background information about bandpass-sampling based receiver radio front-end design. **Chapter 5** presents an introduction to our study on the effects of radio front-end PLL phase noise on GNSS receiver performance. **Chapter 6** describes the state-of-art in GNSS receiver testing. The most important parameters-to-test of a typical receiver are listed, followed by the commonly used procedures for testing each of these parameters. This chapter also describes how these procedures can be adapted for a multi-frequency, multi-constellation receiver testing environment. **Chapter 7** is a summary of the scientific publications emanating from this research work. The manuscript concludes with a summary of the main results and proposals for future work in the continuation of this research direction.

2. BASICS OF GNSS

2.1 Concept of Satellite Positioning

As discussed in Section 1.1, a typical satellite-based navigation system consists of three segments, viz. Space segment, User segment and Control segment. The Space segment consists of man-made satellites revolving in medium-Earth orbits. These satellites continuously transmit digital navigation data modulated on fixed analog frequencies. The User segment consists of electronic receivers that receive signals transmitted by the satellites and extract the digital navigation data which is then used in complex processing algorithms to calculate accurately the position and velocity of the user on the surface of the Earth. The Control segment consists of ground stations that control the movement and well-being of the satellites and also the signals they transmit. The Control segment also monitors the satellites continuously to record their real time 'health' and sends correction data to the satellites in case there is a slight error in their position. Figs. 2.1 [34], 2.2 [35] and 2.3 [36] explain exactly how the three segments work to help a user know his current position velocity and time (PVT) using GNSS.

The satellites transmit accurate timing and self-identification information. This information helps the receiver know exactly when the signal was transmitted (and hence calculate the delay in propagation from the satellite to the Earth) and which satellite transmitted it. The receiver receives such signals simultaneously from all satellites currently visible in the sky overhead. To determine the position of the user, the receiver must compute the solution for four variables: *x, y, z* and *Δt* (3D location and the receiver clock bias). This is performed using the process of trilateration.
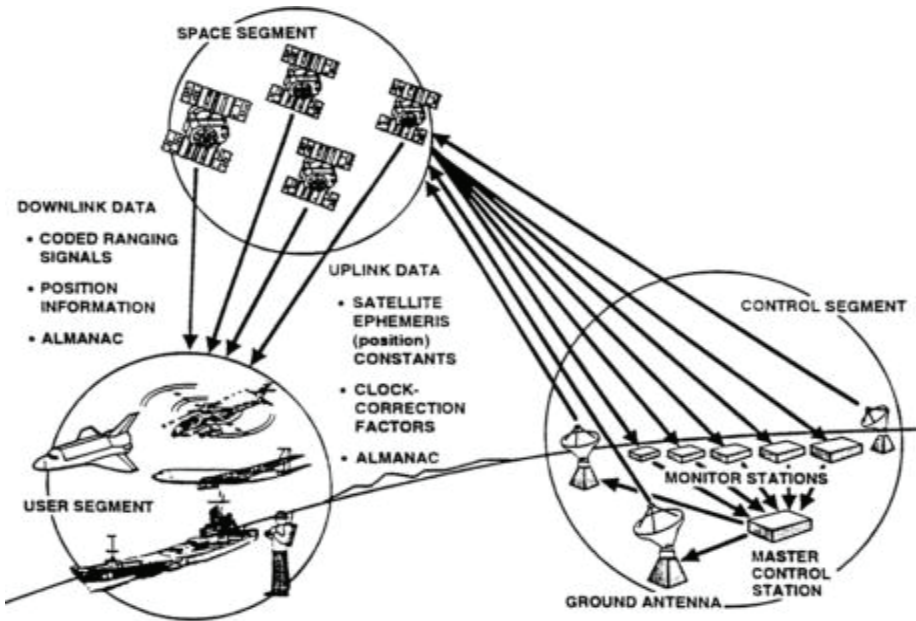
Fig. 2.1 GPS Space, User and Control segments and their inter-relation
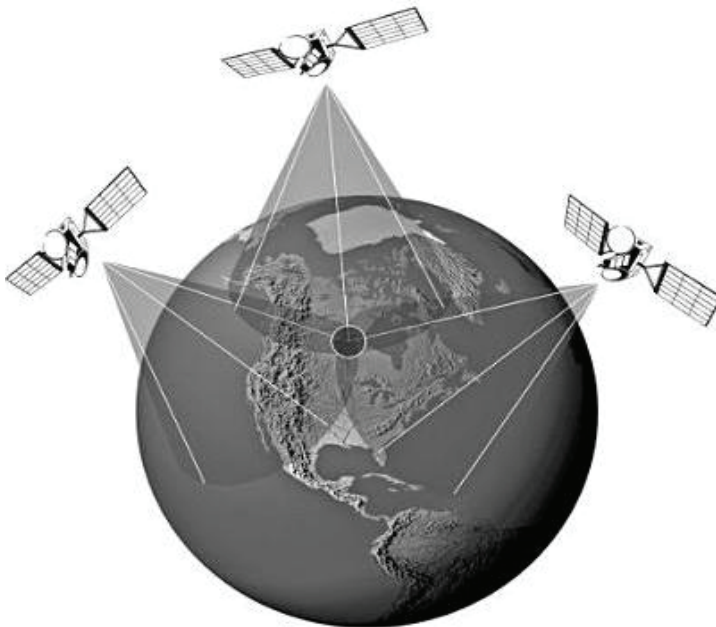
Fig. 2.2 Estimating the position of a receiver by trilateration with three satellites
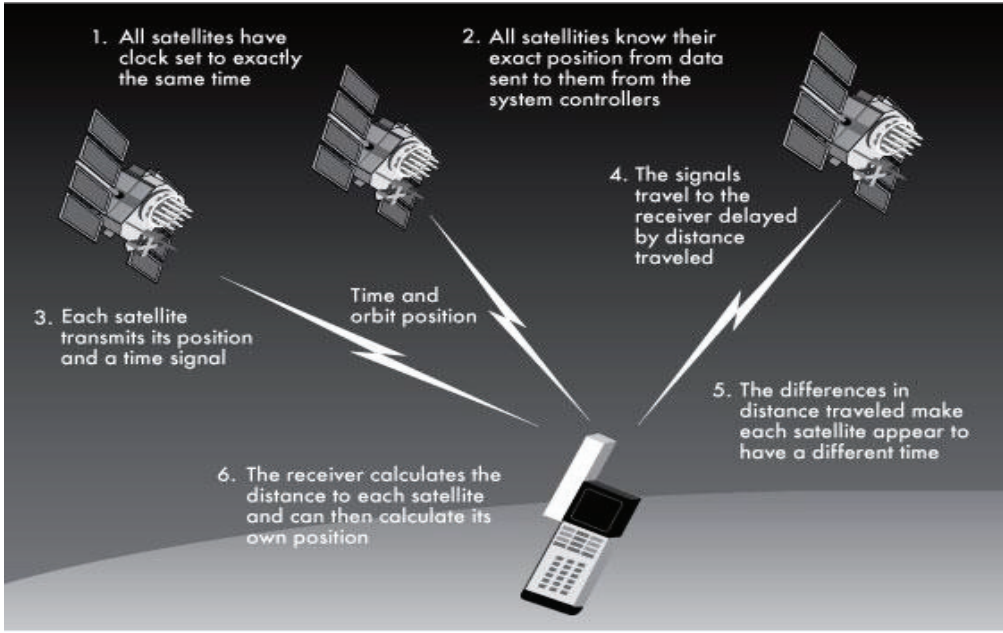
Fig. 2.3 Concept of GNSS operation

The locus of all points equidistant from one 'visible' satellite is a circle on the surface of the earth. Similar circles can be drawn for other 'visible' satellites once their distance from the receiver is measured. The exact location of the receiver is at the point where all such circles meet. Since there are four unknowns, information from four satellites is necessary and enough for estimation of receiver position. The distance between the receiver and one satellite is called the pseudorange. It is expressed by (1) [31]:

$$\rho_s = \sqrt{(x_s - x_u)^2 + (y_s - y_u)^2 + (z_s - z_u)^2} + ct_u \qquad (1)$$

where ρ_s is the pseudorange between one satellite and the user, x_s, y_s, z_s are the coordinates of satellite position, x_u, y_u, z_u are the coordinates of user position, c is a constant that defines the speed of light, and t_u is the offset between satellite system and the user receiver clocks. Once the distance between the user and at least four satellites is established, this information can be used to find the three dimensional position of the user (that is, to solve

11

(1) and determine values for coordinates of user position x_u, y_u, z_u) and solve for time offset between the receiver and satellite clocks.

2.2   GNSS Signal Structure

The various signals and codes that make up the composite GNSS signals vary from one constellation to another, and are described in detail in the following references [37], [38], [39], [40], [41], [42], and shown in Fig. 2.4 here. These references provide considerable information on the structure and description of various GNSS signals, and hence are not discussed again here.

2.3   GNSS Signal Spectrum

Fig. 2.4 [43] shows the overall frequency spectrum of the various satellite-based navigation system signals currently in the planning and/or completion stages throughout the world. As the figure shows, the frequency band of interest is from 1164 MHz to 1615.5 MHz resulting in a total bandwidth of 451.5 MHz. However, there is a 259 MHz band in between Galileo E6 and Galileo E2 (1300 MHz and 1559 MHz) that is not of interest (if we ignore the Galileo search and rescue (SAR) signal at 1544 MHz). Therefore, the entire spectrum of interest can be divided into two sub-spectrums of bandwidth 136 MHz and 56.5 MHz respectively. This relaxes the sampling frequency requirement considerably, as shown in Section 4.

Fig. 2.4 GNSS frequency spectrum

2.4   *GNSS Receiver Structure*

The User segment consists of a GNSS receiver which receives signals from the satellites and/or other sources, e.g., cellular base stations [14]. A block schematic of a typical GNSS receiver is shown in Fig. 2.5 [44].
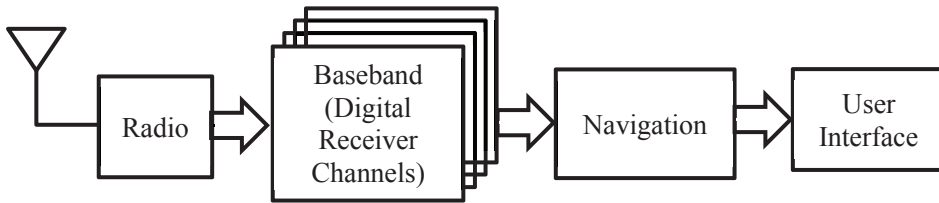
Fig. 2.5 Block diagram of a typical GNSS receiver

The antenna receives the signals from the satellite and forwards them into the analog radio front-end. The radio front-end is responsible for signal amplification, filtering out of band noise, frequency downconversion from RF to an intermediate frequency (IF), and analog to digital conversion. The digitized signal is then passed to the baseband processing unit, where the satellite acquisition and carrier and code signal tracking processes are performed. Acquisition is a process during which the receiver searches for visible satellites in the sky, and when found, the tracking process will keep track of the acquired satellites during their relative motion with respect to the receiver. Tracking the satellite is necessary to be able to demodulate the navigation message from the composite signal and measure pseudoranges for subsequent navigation processing [45], [46], and [47].

2.5   *RF Front-end Architecture Evolution*

Wireless transceiver implementation began with the development of the Monodyne receiver in 1890's, followed by the invention of the Superheterodyne receiver in 1915. Since then, the evolution has been concentrated on developing advanced information modulation and encoding schemes and simultaneously developing hardware and software capable enough to implement these schemes [48], [49]. The current state of wireless

receiver architecture can be described by Fig. 2.6. The evolution of radio transceiver with respect to integration on silicon can be described by the comparative study presented in Table 2.1.
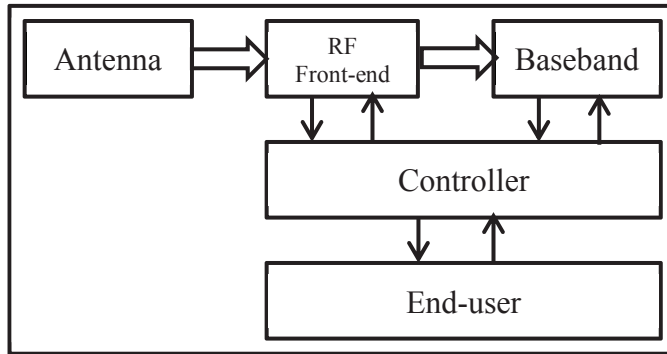
Fig. 2.6 Current state of wireless receiver architecture

Table 2.1 Evolution of radio transceiver with respect to integration on silicon
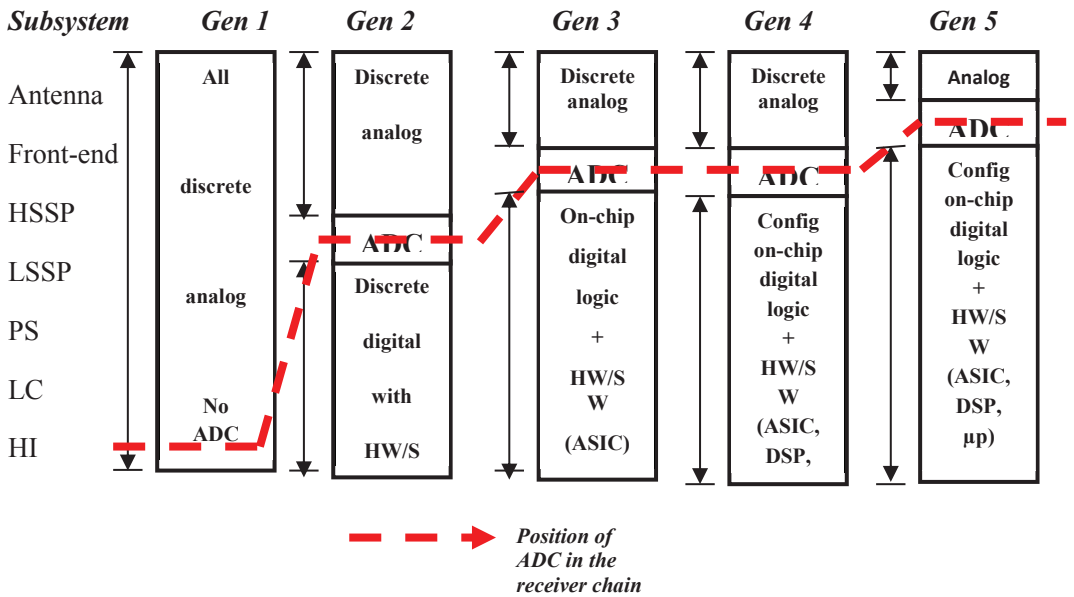
A typical receiver is considered to consist of an antenna, RF front-end, High Speed Signal Processing (HSSP) unit, Low Speed Signal Processing (LSSP) unit, Protocol Stack (PS), Local Control (LC) unit and finally, a Human Interface (HI) unit. One can clearly distinguish a pattern in the evolution; with each new generation, there is an attempt to move the ADC closer to the antenna.

The ideal software defined radio (SDR) architecture is given in Fig. 2.7. In this architecture, the behavior of the radio in the physical layer is defined in software, thus enabling on-the-air software upgrades of the physical layer behavior. Consequently, the analog front-end is configurable to support wide range of frequencies and applications.
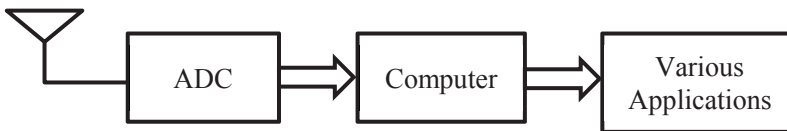
Fig. 2.7 Ideal SDR architecture

2.6   Receiver Radio Front-end Architectures

This section describes briefly the various radio front-end architectures such as direct conversion, superheterodyne, and the direct bandpass-sampling, which are used in typical communications receivers.

2.6.1   Direct conversion Architecture

Direct conversion receivers perform downconversion of the high frequency carrier signal directly to the baseband frequency or zero frequency (also called direct current (DC)), as shown in Fig. 2.8 [50]. It does not contain an intermediate frequency processing stage. Its benefits are reduced component count, better suitability for integration on silicon, and the ease of frequency planning. The most important drawbacks of this architecture are pink noise (flicker or 1/f noise) that usually affects low frequency signals, and local oscillator (LO) leakage creating a DC offset that can potentially drive the successive stages into non-linearity. The Low IF architecture attempts to overcome these disadvantages. It has an IF stage where the RF carrier is downconverted to a non-zero, yet very low IF.
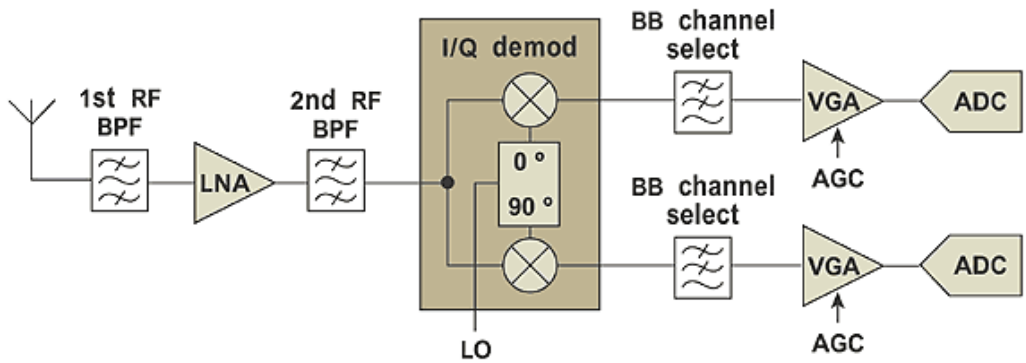
Fig. 2.8 Block diagram of direct downconversion receiver

This ensures that channel selection can be done with highly selective filters and yet the signal is not contaminated by pink noise or DC offset.

2.6.2   Superheterodyne Architechture

In this architecture, the RF carrier signal is first downconverted to an intermediate frequency, usually much higher than the baseband frequency. The benefit of this architecture is that sufficient SNR is maintained, and it is also possible to achieve good selectivity in the IF filters. Drawbacks include, image frequency problems, difficulty to integrate on silicon because of the bulky RF filters, and necessity for complex frequency planning. Fig. 2.9 shows a typical architecture for superheterodyne receivers.
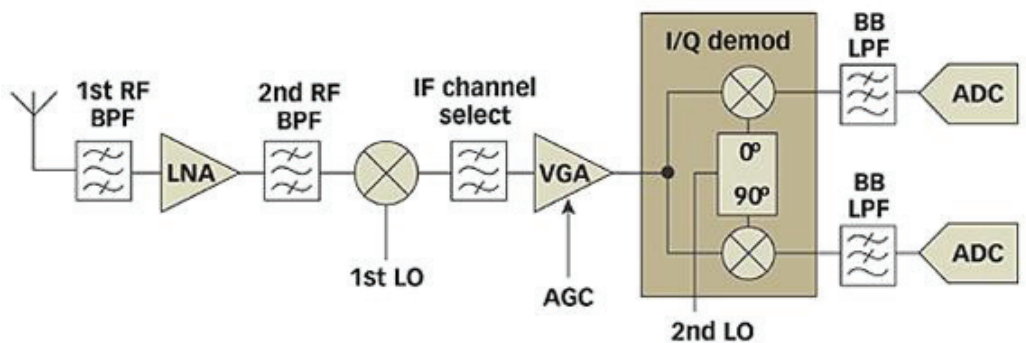
Fig. 2.9 Block diagram for superheterodyne receiver

2.6.3 *Direct Bandpass-Sampling Architecture*

This architecture directly samples the RF signal bandwidth and converts it to digital IF using the principle of intentional, yet non-destructive aliasing. The RF signal from the antenna is filtered to remove any out of band noise, amplified and then directly digitized using a high speed ADC. After the ADC, digital filters are employed to separate the IF bands to be demodulated in the baseband processor. Fig. 2.10 shows the block diagram of a bandpass-sampling RF front-end [51]. The design principle of this architecture is described in detail in Section 4.
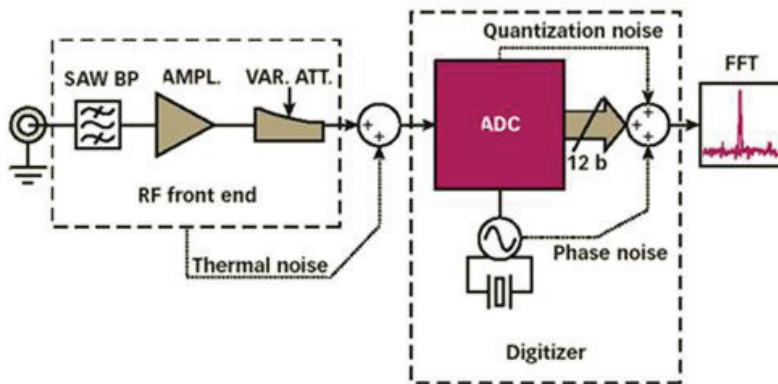
Fig. 2.10 Block diagram of direct bandpass-sampling receiver architecture

3. SOFTWARE-BASED GNSS SIGNAL SIMULATORS

3.1   Introduction and background

Another solution to investigate novel sources for test GNSS signals was to use a software-based GNSS signal simulator. The primary motivation for investigating this solution was the ease with which it could be designed and implemented within the research group without the need for expensive commercial components. This Chapter presents the general introduction to the theory, including an overview of the essential components of such simulators. Publication [P1] extends this discussion by describing a detailed literature review of state-of-art in software-based simulators. This is followed with information about the first results of the TUT's GNSS Signal Simulator in Software (TUTGSSS) developed in the research group using the Matlab programming environment.

GNSS signal simulators are used for imitating the satellite signals arriving at a receiver under test. They provide a deterministic and repeatable source of signals, independent of satellite constellations available and visible at the time of testing [72] – [110]. Simulators have a modular design, where each module is responsible for a particular functionality. The different modules include (but not limited to): The signal generation module, including error signals generation, the transmission channel module, the satellite constellation module, and the receiver RF FE module. Fig. 3.1 shows the block diagram of a typical software-based GNSS simulator. The satellite constellation module gives a real-time view of the geometry of the satellites in the sky. Based on this geometry, signals from the visible satellites are generated at an intermediate frequency and combined to

form a composite navigation signal-in-space, e.g., Galileo E1 or GPS L1. This composite signal flows through the transmission channel module, which simulates non-idealities and other effects, e.g., interference and multipath signals, and additive white Gaussian noise, within a typical transmission path between the satellite and receiver. The RF FE module simulates the effects of the radio frequency front-end of a typical GNSS receiver on the signal received from the sky. This includes filtering, amplification, local oscillator phase noise and ADC quantization effects. The following sections describe the implementation of a simple software-based simulator using the SIMULINK tool.

3.2   Signal Generation Module

The signal generation module is composed of a number of channels, as shown in Fig. 3.2. Each channel simulates one signal, either a legitimate positioning signal or an interference signal, and the various timing errors affecting this signal. The sampled time generator creates time samples from a continuous time source by sampling at a user desired sampling frequency. In the error signal generation block the sampled time is contaminated with various clock errors and atmospheric timing errors. The most common timing errors and their typical values [14], [33] are given in Table 3.1. These typical values are generalizations of the average value of these errors over a long time and wide areas, and may be considered accurate enough only for simple simulators for academic purposes. For higher accuracy, complex mathematical error models are used, which attempt to replicate real-world situations faithfully.

The digital and analog components of the GNSS signal are affected equally but in opposite manner by the ionosphere. It advances the carrier component while delays the code [32]. Hence, there is a need for two time sample streams, called $t_{carrier}$ and t_{code}. These streams are then used in the creation of the digital pseudorandom noise (PRN) code and navigation data, and the radio frequency carrier. To create the digital components, the easiest approach is to create them as memory codes in look-up tables as shown in Fig. 3.3. The $t_{carrier}$ component is used to create the in-phase and quadrature (I/Q) components of the analog high frequency carrier signal, using (2) and (3). Using software tools, it is not possible to handle signals with large sample rates. Hence, it is more convenient to

Signal Generation Module

Channel 1

Channel 2

Channel 3

Satellite
Geometry
Module

Channel 4

Channel 5

Channel 6

Channel n

Transmission
Channel
Effects

Receiver
RF FE
Module

Sampled GNSS Signal at IF

Computer Software Control
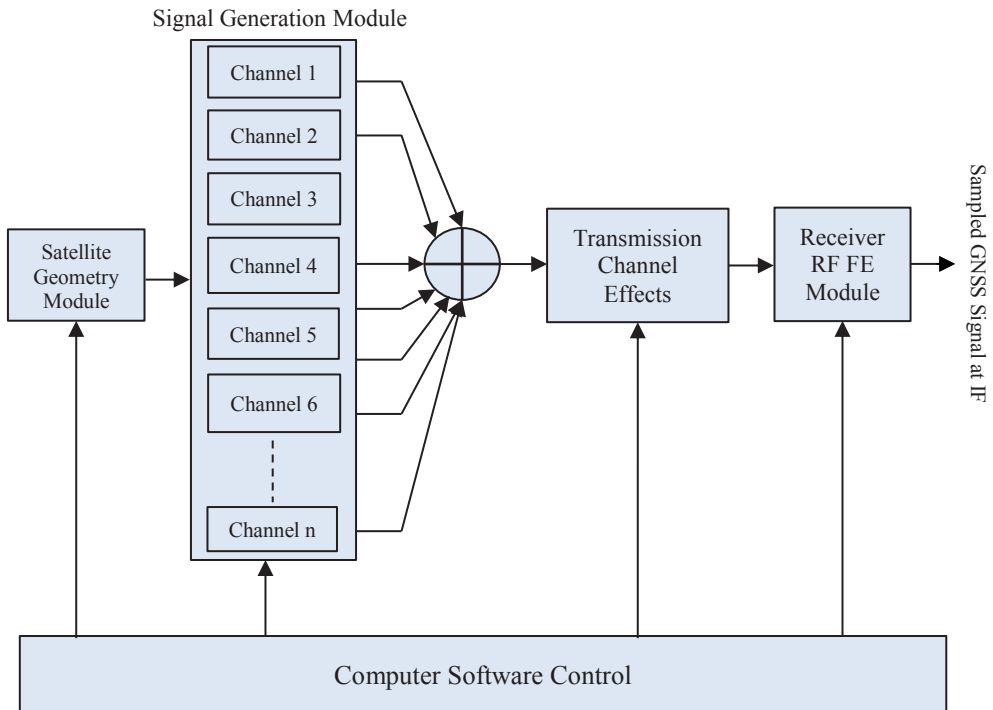
Fig. 3.1 Block diagram of a software-based GNSS signal simulator

Timing Error
Sources

Receiver
Clock Error

Satellite
Clock Error

Sampled
Time
Generator

Pure
Time

Integrated
Doppler
Timing Error

Ionospheric
Delay error

Tropospheric
Delay Error

Timing offset
Error

Time
(with
timing
errors)

GNSS Signal
Generator

Pseudorandom
Code Gnerator

Navigation
Data
Generator

Q

I

Q

I

Band-Limit
Filters

Real-Imaginary
To
Complex
Converter

Channel
Output

90º

Intermediate
Frequency
Carrier
Generator

Fig. 3.2 Internal block diagram of one channel of the simulator

21

Table 3.1 Typical values of GNSS signal errors

Parameter	Typical Value
Receiver clock error	15 ns
Satellite clock error	7 ns
Ionosphere error	17 ns
Troposphere error	2 ns
Timing signal offset error	few ns
Doppler frequency offset	±12 kHz

simulate GNSS signal-in-space at a lower intermediate frequency, e.g., in the range 2 MHz to 5 MHz, rather than the actual 1.5 GHz.

$$I_{carrier} = A\, cos(2\pi f_{carrier} t_{carrier}) \tag{2}$$

$$Q_{carrier} = A\, sin(2\pi f_{carrier} t_{carrier}) \tag{3}$$

3.3   Error Generation Module

The error generation module consists of a number of sources of timing and power variation errors that affect the GNSS signal during its travel from the satellite to the terrestrial receiver, and also within the receiver signal processing chain. Here, we explain the most common error sources, e.g., receiver and satellite clock errors, atmospheric delay errors, transmission channel effects and radio front-end effects. The accuracy of the signal simulator is directly dependent on the number and sophistication of the error sources that it can model.

3.3.1   Receiver Clock Error

The time offset between the receiver's clock and the standard GPS (or Galileo) time is called the receiver clock error. Receiver clocks are usually constructed using crystal oscillators, which suffer from higher rates of drift yet are more affordable than the ultra-

22
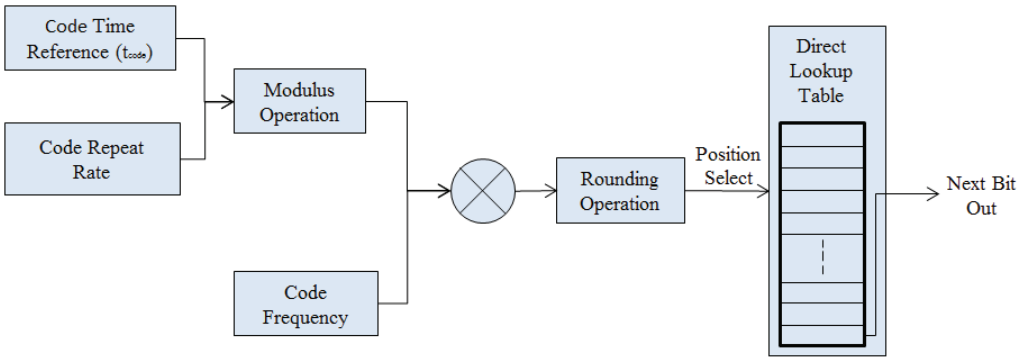
Fig. 3.3 Simulink model for generating Galileo E1B primary PRN code

stable atomic clocks used in the GNSS satellites. The receiver clock error is a combination of systematic and random errors [2]. Examples of systematic errors are the constant time and frequency offsets, defined in units of parts per million (ppm). The Allan Variance (AV) [3] commonly characterizes the remaining frequency errors. The AV gives the measure of frequency instability of the clock over consecutive samples. Using M samples, AV can be modeled by (4) [4]:

$$AV(\tau) = \frac{1}{2(M-1)} \Sigma_i (y(\tau)_{i+1} - y(\tau)_i)^2 \tag{4}$$

where τ is the time period over which AV is calculated and $y(\tau)_i$ is the ith sample value.

3.3.2   Satellite Clock Error

The time offset between the satellite's clock and standard GPS time is called the satellite clock error. Satellites have highly accurate and precise atomic clocks, with small frequency drift. The ground control segment monitors this drift at regular intervals and a correction parameter is transmitted by the satellites through the navigation message. Navigation messages transmitted by the satellites are available on the internet [5] in various file formats such as YUMA, SP3, and RINEX. Historical values of the satellite clock correction parameter can be studied using these files, and with reverse-engineering, the satellite clock error can be modeled. As an alternate, URA/SISA parameters [6], [7]

can be used to model the satellite clock errors in a similar way. The equation for the satellite clock error is given by (5) [8].

$$dt = a_0 + a_1(t - t_{oc}) + a_2(t - t_{oc})^2 \qquad (5)$$

where t_{oc} is the reference epoch in seconds, a_0 is the satellite clock time offset in seconds, a_1 is the fractional satellite clock frequency offset and a_2 is the fractional satellite clock frequency drift.

3.3.3   Ionospheric Delay Error

The ionosphere is the outermost layer of the atmosphere, lying between 50 km to more than 1000 km from the Earth's surface. This layer consists of free ions which collide with the electromagnetic waves of the GNSS signals passing through it, causing the waves to refract or bend. This introduces a time error in the carrier and the code components of the signal. This error is highly dependent on the signal frequency and on the number of free ions in the ionosphere. A parameter that gives information on the current condition of the ionosphere is the Total Electron Content (TEC). The value of TEC is dependent on the geographic location of the receiver and the time of day. TEC values over a particular area and at a particular time of day are available from the internet [9]. These TEC values can be used to model the ionospheric errors.

Usually for GPS, the Klobuchar model is used using the 'ION ALPHA' and 'ION BETA' parameters from GPS RINEX files available on the internet [10]. For Galileo signals, the NeQuick model is preferred, which builds on the formulation for the electron density function in the Epstein layer of the ionosphere given by (6) [11]:

$$n(h) = \frac{4n_{max}}{\left(1+exp\left(\frac{h-h_{max}}{B}\right)\right)} exp\left(\frac{h-h_{max}}{B}\right) \qquad (6)$$

where $n(h)$ is the electron density at height h, n_{max} is the peak electron density, h_{max} is the height of peak electron density, and B is the thickness of the layer. Once the electron

density in the ionosphere above the receiver is computed, it can be used to calculate the delay and phase errors affecting the various satellite signals passing through it.

3.3.4 Tropospheric Delay Error

The troposphere is the layer of atmosphere up to 20 km from the Earth's surface. This layer also introduces delays in the GNSS signal propagation but unlike the ionosphere, this delay is independent of signal frequency. There are many models to simulate the troposphere. However, the most popular is the Modified Hopfield model, which is based on a model for the wet and the dry zenith tropospheric delays and a slant delay transformation. The equation for tropospheric error (in meters) using this model is given by (7) [12]:

$$dTropo^{MH}\big(P(t), T(t), H(t), El(t)\big) = dTropo^{GG}\big(P(t), T(t), H(t), El(t)\big) + w \qquad (7)$$

where $dTropo^{GG}$ is the slant tropospheric delay (in seconds) generated using the Goad and Goodman tropospheric model, $P(t)$ is time variant pressure parameter, $T(t)$ is time variant temperature parameter, $H(t)$ is time variant humidity parameter, $El(t)$ is elevation angle, and w is Gaussian white noise. An alternate equation for tropospheric error (in meters) is given by (8) [8]:

$$T_r^S = 10^{-6} \int_a^b N ds \qquad (8)$$

where $N = (n-1)*10^6$ is the refractive index along the signal path and a and b define the limits of tropospheric boundary in meters. Increased accuracy of modeling the atmospheric errors is possible if the obliquity factor is included. However, in that case the signal generation module needs to take into account the satellite geometry and user position information into the error generation [13].

3.3.5 Doppler Frequency Offset

Doppler phenomenon is the change in frequency of a signal incident upon a target from a source, one or both of which are in motion. The signal frequency changes at a rate which

is dependent on the speed and direction of relative motion between them. The usual range of Doppler offset in GNSS signals is about ±12.5 kHz. This includes the satellite relative velocity, the receiver clock frequency offset, and the receiver velocity [14]. The PRN code frequency is also affected by the Doppler offset, but since this frequency is much lower than the RF carrier frequency, the offset will be much smaller - typically in the order of a few Hz. If the receiver is able to accurately identify the amount of this Doppler offset, the relative velocity, acceleration and jerk between the receiver and satellite can be determined.

From a simulator point of view, altering the carrier and code frequency of every channel within their respective ranges stated above and based on the satellite positions and trajectories, a Doppler offset can be introduced into the simulator output. An additional Doppler offset would help to simulate receiver motion. Therefore, by a right combination of Doppler frequencies over different intervals of time, a dynamic (receiver-in-motion) scenario can be simulated.

3.4 *Transmission Channel Module*

The internal block diagram of the transmission channel module is shown in Fig. 3.4. Three errors that are typically introduced in this module are interference and multipath signals, and additive white Gaussian noise (AWGN). More than one channel can be dedicated to simulating the interference and multipath signals, usually from the left-over channels from the Signal Generation module. Interference signals are characterized by the modulation type (e.g. FM, AM, DVB etc.), frequency offset from the GNSS signal-of-interest, and the signal power. Important parameters in the case of Multipath error are the number of multipath components, and the magnitude and the delay (in samples) of each component with respect to the fundamental component. AWGN can be generated as random noise with zero mean, and variance equivalent to the maximum noise power required to maintain the carrier to noise ratio (CNR) defined for each channel. The basic function of the transmission channel for the Galileo E1 signal in terms of the sub-carrier can be modeled as shown in (9).

$$r_{E1}(t) = \sum_{i=1}^{l} \alpha_i(t)\, S_{E1}(t - \tau_i) + n \tag{9}$$

where $r_{E1}(t)$ is the Galileo E1 received signal after the transmission channel, α_i and τ_i are the complex path coefficient and path delay for the ith path respectively, and n is the AWGN.

3.5 *Radio Frequency Front-End Module*

Some state-of-art software simulators have the capability to model different antenna patterns and signal power profiles [15]. Typically though, only RF filtering effects, amplification, and analog to digital (ADC) conversion losses are considered. The RF filter is similar to the band-limited filter used in each channel of the signal generation module, as shown in Fig. 3.2. The filter bandwidth depends upon the signals being received. The various filtering effects that can be simulated include band-limiting, insertion loss, passband ripple and group delay. The low noise amplifier includes gain and noise figure effects. Simulating noise figure is equivalent to introducing additional AWGN before the output of the amplifier. ADC quantization causes degradation in signal to noise ratio (SNR) of the received signal [16]. Additionally, an important contribution of this thesis work is to demonstrate how to include the effects of phase noise from the radio front-end's local frequency generator within the received signal [P4], [P5], [P6].

3.6 *Satellite Geometry Module*

The satellite geometry module is responsible for controlling the individual channels according to the currently visible satellite positions and trajectories. The signal strength and pseudorange are controlled depending on the elevation angle of the satellite, while the Doppler frequency offset is decided based on the rate of change of pseudorange, which is based on direction of satellite motion with respect to the simulated receiver position. Publication [P1] describes the solutions and techniques used by state-of-art software-based GNSS simulators in simulating the satellite geometry. They answer important questions such as, from where does this module get the current (real-time) picture of the satellite positions and trajectories in the sky? What are its inputs and which data-formats are supported?

Interference Signal Generation

Input from Signal Generation Module

Channel 1
Channel 2
Channel 3
Channel 4
Channel 5
Channel 6
Channel 7
Channel 8

Multipath

Additive White Gaussian Noise

Output of the Transmission Channel Module

Multipath Components with Magnitude and Delay

LOS Component

Multipath 1 — Delay 1
Multipath 2 — Delay 2
Multipath 3 — Delay 3
Multipath 4 — Delay 4

Fig. 3.4 Internal block diagram of transmission channel module

4. BANDPASS-SAMPLING BASED GNSS RECEIVER RF FRONT-ENDS

4.1 Introduction and background

One of the solutions proposed towards investigating novel sources of test signals for GNSS receivers was a bandpass-sampling based radio front-end capable of processing all planned GNSS signals, called here the Sampled Data Generator (SDG). As defined in Section 2.3, the composite bandwidth of the GNSS signals extends from 1164 MHz to 1300 MHz, and from 1559 MHz to 1615.5 MHz, and is shown in Fig. 4.1 [115]. The bandpass-sampling architecture is built around the concept of direct digital conversion of a band of RF frequencies using a wideband ADC, followed by channel selection in the digital domain using digital filters. The ADC is a critical element and some of its desirable properties for this particular application are high speed, low jitter, low power consumption and low resolution. Publications [P2] and [P3] describe in detail the background literature study about general theory of wide-bandwidth sampling, and previous cases of its implementation in the GNSS domain. Here we briefly present some of the essential components of such radio front-ends (please refer to Fig. 2.10), which include the antenna, low noise amplifier, and RF Filter and ADC for the actual bandpass-sampling.

4.2 Antenna

The antenna to be used for this architecture would need to be wideband, capable of receiving signals from 1164 MHz up to 1615.5 MHz. We propose here, few good commercial antenna options, e.g., the Zephyr 2 and Zephyr Geodetic 2 antennas from

Trimble [52], Satellite Navigation Antenna from Roke Manor Research [53] and Universal GNSS Antenna designed at the Wang Electro-Opto Corporation (WEO) [54].

4.3   Low Noise Amplifier (LNA)

The antenna is connected to a low noise amplifier using a 50 Ohm interface. A low noise amplifier is a device that amplifies incoming signals while introducing little noise of its own. Because of this property (high amplification but low noise injection), it is usually placed as the first component in a receiver chain. According to Friis' formula for overall noise factor of a receiver chain, the first component's noise and gain heavily influence the overall noise factor of the receiver chain [55], [56], [57]. Publication [P2] describes the design and implementation of an LNA within the Sampled Data Generator, capable of operating on the entire GNSS frequency band of interest. It also describes the design and software simulations of RF filters and the bandpass-sampling ADC, used subsequent to the LNA stage.
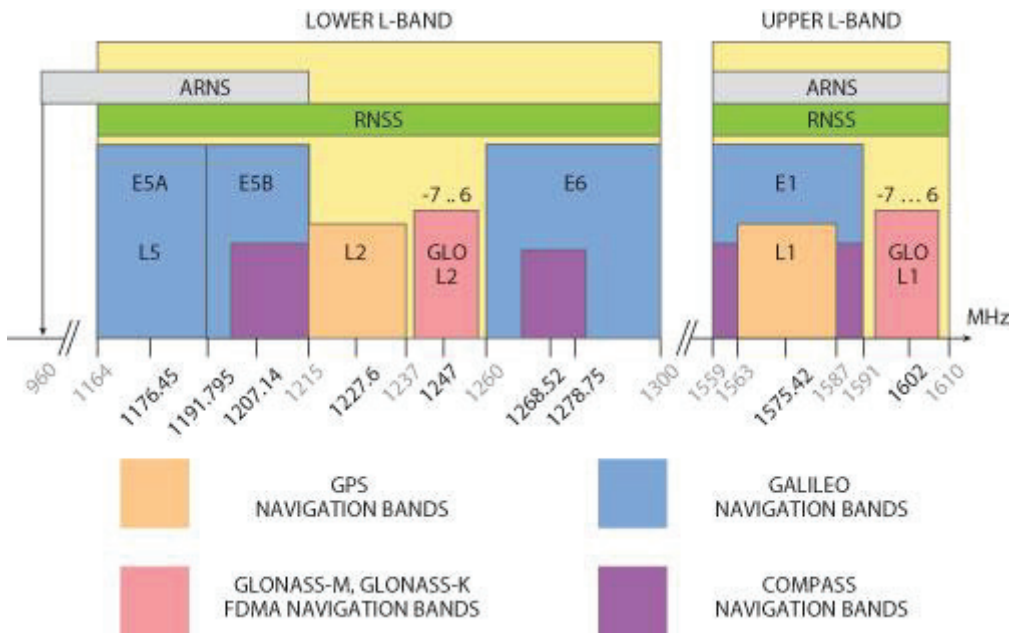
Fig. 4.1 Frequency spectrum of the proposed SDG

4.4   RF Filter

To isolate the two GNSS bands as stated in Section 3.1, it requires one RF bandpass filter (1164 MHz to 1615.5 MHz) followed by an RF bandstop filter (1300 MHz to 1559 MHz). These filters were designed as seventh-order LC Chebyshev filters in order to trade-off sharpness of filter cut-off with complexity and cost of final design. The design methodology adopted was as follows: first, the seventh-order low pass Chebyshev filter was designed, followed by the transformation from low pass to bandpass or bandstop filter using the principle of component transformations. Publication [P3] describes the design and simulation results of these two filters in detail.

4.5   Direct RF bandpass-sampling

The primary concept of direct bandpass-sampling based GNSS receiver front-end is to achieve digitization of the complete RF band of interest into digital intermediate frequency, thus eliminating the need for an analog mixer. The following describe the numerical analysis of this method, its benefits and drawbacks. The following research papers [58] - [71] are cited as references in support of this discussion, and are listed in the reference section of this thesis work. More details are provided in the Publication [P3].

4.5.1   Concept and numerical analysis

Upon sampling of a band of frequencies, the resulting spectrum consists of the original band replicated at integer multiples of the sampling frequency as shown in Fig. 4.2. Furthermore, to avoid any destructive aliasing (Fig. 4.3) it is necessary to sample at a frequency greater than twice the bandwidth (Fig. 4.4). This relaxes the sampling frequency requirement and also does not compromise on the data content in the sampled output.

ORIGINAL   SAMPLED
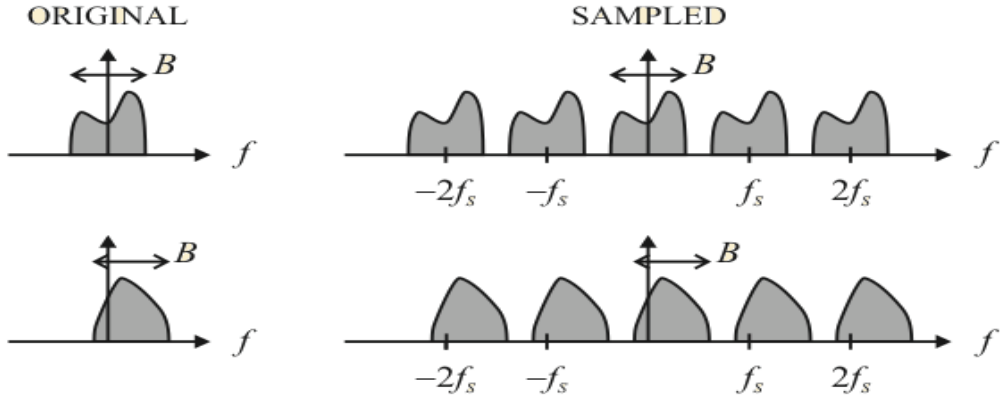
Fig. 4.2 Frequency spectrum of a complex signal before and after sampling
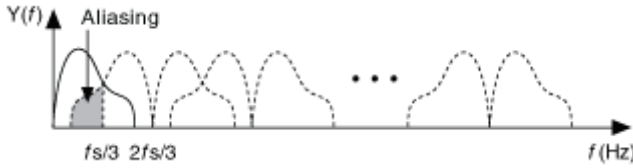
Fig. 4.3 Frequency spectrum showing harmful aliasing between different IF bands
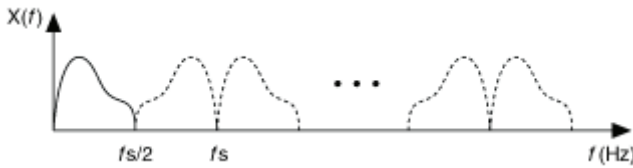
Fig. 4.4 Frequency spectrum showing different IF bands without aliasing

For a set of two real distinct bands (as in the case of the proposed SDG), appropriate sampling frequency can be computed based on the simultaneous fulfillment of certain conditions as given by (10) to (17).

Bandwidth of interest = *(1300 MHz – 1164 MHz) + (1615.5 MHz – 1559 MHz)*

= *192.5 MHz* (10)

$$\text{Center frequency of band 1 } (f_{c1}) = 1232 \text{ MHz} \tag{11}$$

$$\text{Center frequency of band 2 } (f_{c2}) = 1587.25 \text{ MHz} \tag{12}$$

$$\text{Minimum sampling frequency } (f_{smin}) = 2*(\text{Bandwidth of interest}) \tag{13}$$

$$\text{Intermediate frequency } (f_{IFi}) \begin{cases} = Rem\left(\frac{f_{ci}}{f_s}\right) & \text{if } Int\left[\frac{f_{ci}}{\frac{f_s}{2}}\right] = even \\ \\ = f_s - Rem\left(\frac{f_{ci}}{f_s}\right) & \text{If } Int\left[\frac{f_{ci}}{\frac{f_s}{2}}\right] = odd \end{cases} \tag{14}$$

$$f_{IFi} > \frac{BWi}{2} \tag{15}$$

$$f_{IFi} < \frac{f_s - BWi}{2} \tag{16}$$

$$|f_{IF1} - f_{IF2}| \geq \frac{BW_1 - BW_2}{2} \tag{17}$$

where *Int[x]* is largest integer smaller than or equal to *x*, and *i* = The frequency band number (Band 1 = 1164 MHz to 1300 MHz and Band 2 = 1559 MHz to 1615.5 MHz). Further computation of possible sampling frequencies is described in Publication [P3]. If the GNSS signals are converted into complex/analytic by using Hilbert transformer and then sampled, the sampling frequency requirement is further relaxed. Fig. 4.5 shows the frequency spectrum of two complex signals with all important frequency points marked on the diagram.

Fig. 4.5 Frequency spectrum of two complex RF signal bands

Equations (18) to (21) give the criteria that must be simultaneously satisfied by the sampling frequency in case of complex GNSS signals.

$$n_1 \leq Int\left[\frac{f_{c1}}{BW_1 + BW_2}\right] \tag{18}$$

$$Int\left[\frac{n_1 * f_{c2}}{f_{c1}}\right] \leq n_2 \leq Int\left[n_1 * \left(\frac{f_{c2}}{f_{c1}}\right) + \frac{f_{c2}}{f_{c1}}\right] \tag{19}$$

$$\frac{f_{H2} - f_{L1}}{n_2 - n_1 + 1} \leq f_s \leq \frac{f_{L2} - f_{H1}}{n_2 - n_1} \tag{20}$$

$$\frac{f_{H2} - f_{L1}}{n_2 - n_1} \leq f_s \leq \frac{f_{L2} - f_{H1}}{n_2 - n_1 - 1} \tag{21}$$

Equation (20) should be used if the position of the resulting sampled bands should be as shown in Fig. 4.6. While if their positions should be as in Fig. 4.7, then (21) should be used. The solid trapezoid denotes spectra of original signal and the dashed trapezoid denotes a replica after sampling the original band.
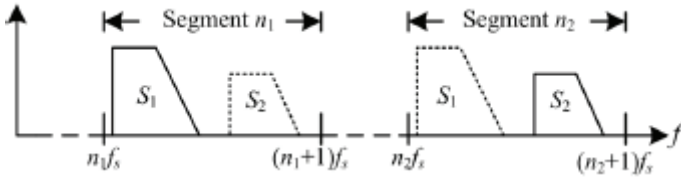
Fig. 4.6 First possibility of arranging the sampled and original bands
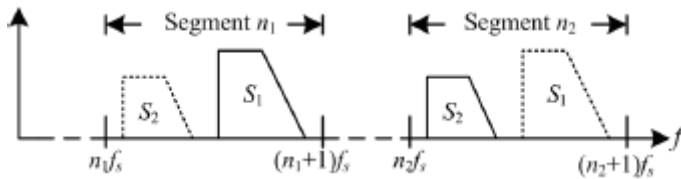
Fig. 4.7 Second possibility of arranging the sampled and original bands

Thus the procedure for obtaining a range of valid sampling frequency for two complex RF signals is: first, choose an appropriate n_1 using (18); next, choose an appropriate n_2 using (19), and last, using (20) or (21) compute the range of sampling frequencies. Equation (22) gives the new position of the sampled IF band when complex GNSS signals are considered.

$$f_c^m = m*f_s + rem(f_c, f_s) \qquad\qquad for\ (m = 0, \pm1, \pm2, \pm3.......) \qquad\qquad (22)$$

where f_c^m is the center frequency of the mth replica of the sampled band, and $rem(f_c, f_s)$ is the remainder from the ratio of f_c and f_s. A drawback in the case of complex signal processing is the need to replicate the ADC in both the signal branches (I/Q), as shown in Fig. 4.8.
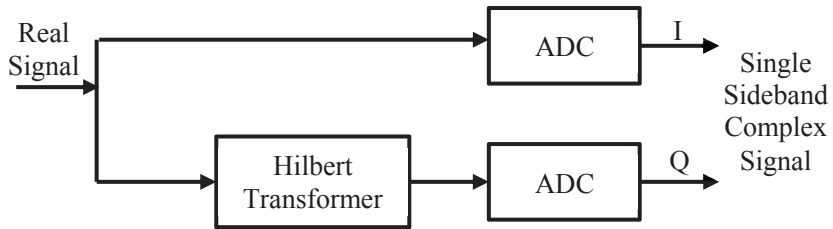
Fig. 4.8 Block diagram of complex bandpass-sampling

4.5.2   Benefits

Using the bandpass-sampling technique, a band of frequencies may be sampled at a rate that is twice the bandwidth, rather than twice the highest frequency component. This offers considerable relaxation in the sampling frequency requirement through the process of non-destructive aliasing. This also eliminates the need for a separate analog mixer. The intermediate frequencies are in digital domain and hence can be separated by digital filters instead of expensive and bulky analog channel select filters. This in turn helps in placing the ADC as close as possible to the antenna, a primary requirement of true software defined radio architecture.

4.5.3   Challenges

There are a number of challenges that must be analyzed and overcome to design a bandpass-sampling receiver front-end architecture.

ADC dynamic range and spurious free dynamic range - due to the wide bandwidth requirement, it is possible that there is considerable difference in the strengths of the signals received at different frequencies within this band. This complicates the decision about the ADC resolution and consequently, also complicates the estimations of the quantization noise. If a low resolution ADC is used, any high power frequency components will be 'clipped'. Such clipping in turn, produces spurious frequency components in the spectrum of the sampled signal.

SNR degradation due to noise aliasing - during bandpass-sampling, out of band noise from around integer multiples of sampling frequency is also aliased onto the desired frequency band after digitization [67]. This causes the degradation in SNR, and this degradation is proportional to the sub-sampling factor as given by (23). A solution to this degradation in SNR due to noise aliasing is to have sufficient amplification in the initial stages of the RF front-end.

$$Sub\text{-}sampling\ factor = \frac{f_{center}}{f_{sampling}} \tag{23}$$

SNR degradation due to clock jitter – The quality of the sampling clock is a major concern as the bandwidth to be digitized increases. In [117] and related works for example, the authors have performed a theoretical analysis of the power of the jitter noise, and the consequent degradation in the signal to noise ratio. Based on this study, a relation for jitter threshold in terms of the useful signal frequency, oversampling factor and power of any possible interferers was proposed. A set of acceptable sampling rates sufficient for Galileo reception were then computed based on this jitter threshold.

Analog to digital conversion is a computationally heavy process - Therefore, the ADC is a bottle-neck in the entire receiver front-end chain, especially for the bandpass-sampling architecture. It consumes most of the time and power allocated to the front-end and in the process generates a lot of heat that can be self-destructing if not dissipated effectively. For this reason, the ADC should have high speed of operation, low power consumption, and yet be affordable. Additionally, it needs to be carefully cooled to keep its temperature during operation within the safe operational limits [69]. The flash ADC architecture offers the fastest conversion speeds. Their only limitations are lower resolution and higher costs. For GNSS applications, lower resolution is not a primary concern and therefore, the flash architecture is worth further investigation in spite of the higher costs involved [68].

5. EFFECTS OF PHASE NOISE ON GNSS TRACKING PERFORMANCE

5.1   Introduction and Background

One of the objectives of this thesis work was to propose novel methods to improve the diversity of receiver characterization. This study proposes a new perspective for GNSS designers, which quantifies the performance loss in the baseband signal's correlation product due to phase noise from the radio front-end frequency source. These performance bounds may then be used as the basis for local oscillator design. Extensive simulations are used to validate results, while drawing conclusions regarding the relationship between phase noise, correlation time, and loss in the carrier-to-noise ratio. The experimental setup is shown in Fig. 5.1.

This Chapter is an introduction to the results provided in Publications [P4], [P5] and [P6], which describe this relationship, first for a free running oscillator case, and then for the more realistic PLL scenario. The actual phase noise models of the free running oscillator and PLL are described in the publications. Here we only provide a brief overview of the study and present some of the intermediate results using a recreation of the simulation scenarios described in the publications.

5.2   Basics of Phase Noise

In typical GNSS receivers, the signal received from a satellite is compared with an internally generated replica of its corresponding code at different code phases until the correlation product is maximized. This provides an indirect measurement of the pseudo-
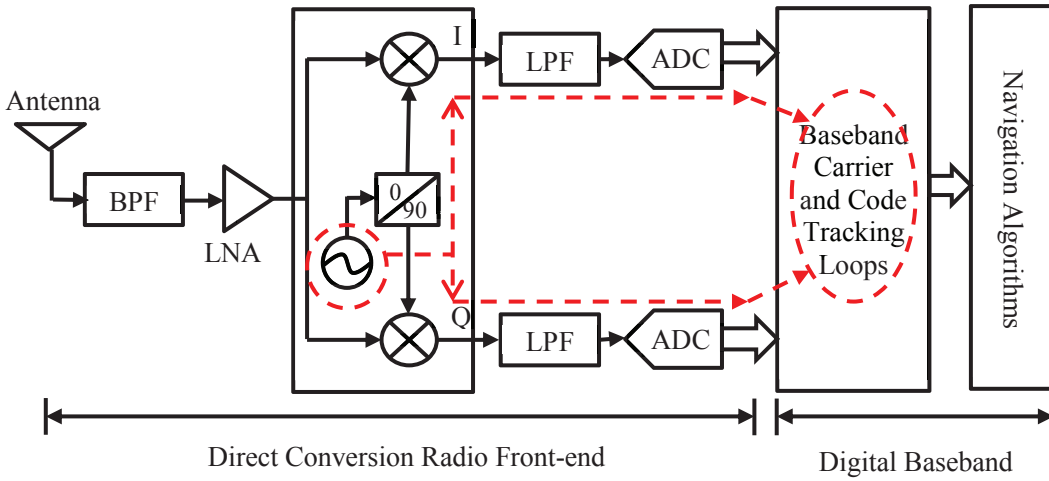
Fig. 5.1 Experimental set-up to study the effect of phase noise on banseband tracking performance
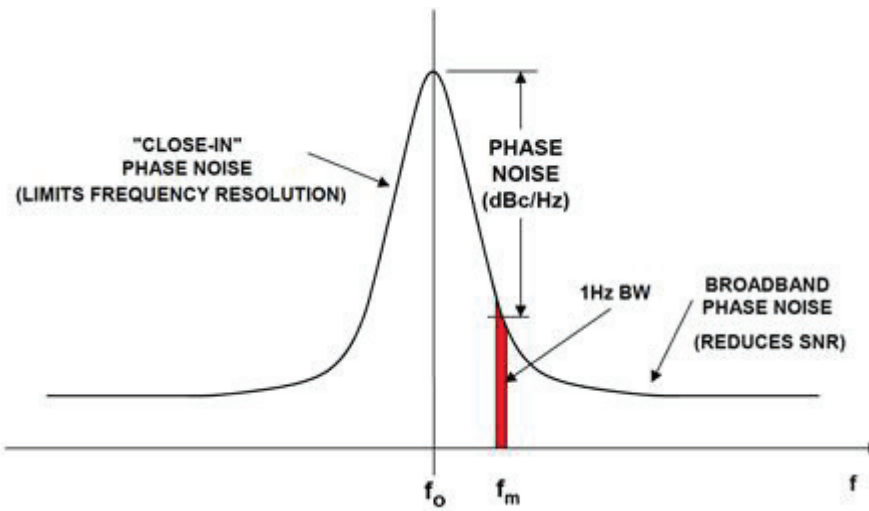
Fig. 5.2 Definition of phase noise

range between the receiver and the satellite. One of the performance limiting factors of GNSS receivers is the imperfection of the radio frequency (RF) oscillator, often referred to as phase noise. Phase noise is the random, rapid short-term phase fluctuations of the radio front-end's local frequency generator [27]. As shown in Fig. 5.2 [83], the phase noise is measured in a bandwidth of 1 Hz at a defined frequency offset from the center frequency. The unit for measuring the phase noise is dBc/Hz. The normalized single side-band phase noise spectral density is given by (24) [28].

$$N_{Phase}(dBc/Hz) = 10log_{10}[\frac{2KT}{P_{Signal}} * (\frac{\omega_0}{2Q\Delta\omega})^2] \tag{24}$$

where N_{phase} is the phase noise within the bandwidth of 1Hz at a frequency offset of $\Delta\omega$, K is the Boltzmann constant of 1.38 x 10-23 J/K, T is the Temperature in Kelvin, P_{signal} is the power of the signal under consideration (in absolute values), ω_0 is the center frequency of the signal under consideration in radians/sec, and Q is quality factor of the resonator in the local oscillator.

The receiver oscillator phase noise adversely affects the frequency down conversion and analog to digital conversion processes, thus diminishing the achievable carrier-to-noise ratio (C/No). Consequently, the correlation outputs in the code-tracking loop and the carrier phase tracking jitter are also adversely affected. Furthermore, longer integration intervals can make integration (correlation) comparatively less effective in the presence of this phase noise. In this study, we attempt to investigate the answers to the following questions: What is the maximum acceptable phase noise level as required by an RF designer in order to achieve a minimum pre-defined C/No? How do correlation losses relate to phase noise levels? Answers to these questions will ultimately help in justifying the addition of this phenomenon in the overall characterization of GNSS receiver performance.

5.3   Simulation Scenarios

In the first part of this study [P4] and [P5], we proposed an analytical approach using a mathematical phase noise model for a simple free running oscillator. Our results provided

a first estimate of the noise floor requirements for a receiver given a particular baseband implementation. However, the FRO model is not well suited to represent practical receiver frequency synthesizers and hence, its direct use for specification of receiver designs is not appropriate. Therefore, the second part of this study [P6], presented the subsequent observations of receiver performance by utilizing the PLL as a practical frequency synthesizer. The results reveal that, there are both quantitative and qualitative differences in performance when compared to the FRO scenario. Here we present a summary of the study in [P6] and show some intermediate results which are then refined and extended in the publication.

The PLL model shown in Fig. 5.3 was used to create sampled phase noise signal vectors (called 'realizations') of duration 200 ms each. These signal vectors were created for different combinations of a range of typical GNSS front-end PLL parameters, as described in Table 5.1. This allowed studying the effect of each PLL parameter upon the GNSS baseband correlation performance. One hundred such realizations were generated for every combination so that the results could be averaged over a considerable size of data samples. The overall PLL phase noise is dependent on the sum of phase noise contributions of its constituent blocks. The contribution of each block is in turn dependent upon various parameters, as shown in Table 5.1. In each realization, only one parameter was varied while keeping all others constant, so that the effect on code correlation due to that parameter (and hence due to that constituent block) could be studied. The method for adding the PN into the signal stream is shown in Fig. 5.4.

5.4   Simulation Results

Fig. 5.5 shows how the SNR of correlation peak degrades with increasing thermal PN of the PLL VCO for different loop filter bandwidths, frequency division ratios (FDR, denoted by N) and PIT values while Fig. 5.6 shows the relation between phase component of correlation peak and the PLL PN. As mentioned earlier, these results are refined and extended in publication [P6].
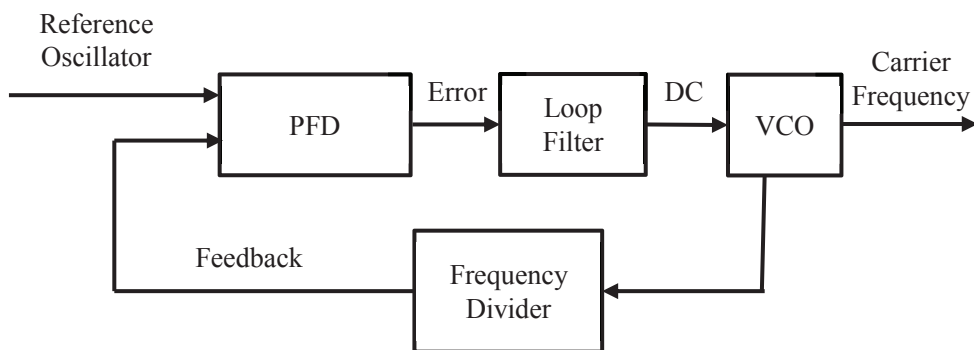
Fig. 5.3 Phase Locked Loop Block Diagram

Table 5.1 Constituent blocks of a PLL and typical values of their significant design parameters

Constituent Block	Important Parameter	Typical Value(s)/Range
Crystal RO	PN (at 10 kHz offset)	-150 dBc/Hz
PFD	PN (at 1 MHz offset)	-265 dBc/Hz
Loop Filter	Order	2nd order
	Bandwidth	1 kHz → 100 kHz
VCO	PN (at 1 MHz offset)	-130 dBc/Hz → -100 dBc/Hz
FD	Division Ratio (N)	64, 200
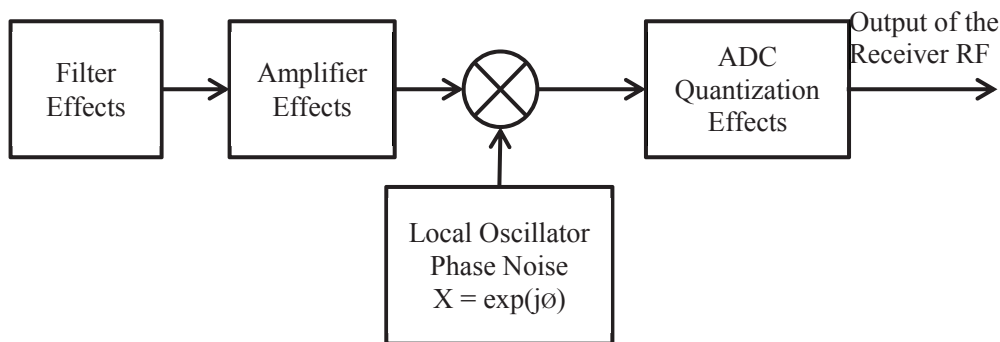
Fig. 5.4 Block schematic showing the mechanism to add phase noise in the signal stream

5.4.1 SNR of correlation peak versus VCO PN

Fig. 5.5 shows that the SNR of correlation peak degrades with increasing thermal PN of the PLL VCO. This degradation is more rapid at higher PLL bandwidths and is approximately 10 dB per every 5 dBc/Hz increase in PN. It should be noted that, the SNR values obtained here are greater than those observed in typical GNSS receivers because the simulation environment does not assume any receiver thermal noise floor. Consequently, this makes the noise-free post-correlation SNR to be infinite.

The dynamic range of the SNR extends from 0 dB to 110 dB for the chosen range of PLL BW and VCO phase noise values; however, its absolute value for a given PN is inversely proportional to the loop filter bandwidth. Therefore, loss in SNR due to PN can be at least partially compensated by increasing the filter BW. This observation is expected, as the VCO PN contribution to the overall PLL PSD is diminished for higher bandwidths. However, there is a limit to which the increase in bandwidth translates to an improvement in SNR. Very large PLL bandwidths would also result in more noise and spurious signals flowing into the signal stream, thus adversely affecting the baseband correlation SNR.

Additionally, increasing the PLL bandwidth propagates the reference oscillator (RO) PN to the output PLL PN, thus making it the bottleneck for improving the SNR. This phenomenon can be observed in the case where both, bandwidth and PIT are large. Comparison between the two frequency division ratios shows that the slope of degradation

remains similar, but there is a noticeable degradation in SNR for a given PN if the FDR is increased to 200. The SNR may even drop to zero in case of small filter BW and high PIT.

5.4.2   *Phase component of correlation peak versus VCO PN*

The objective is to maintain the standard deviation of phase angle of the correlation result over consecutive epochs below 10 degrees so that the tracking loop PLL can keep track of the correlation product. Fig. 5.6 shows that, although increasing VCO PN degrades the phase angle stability, this degradation is not significant for bandwidths greater than 5 kHz. GNSS radio front-end PLLs usually have filter bandwidths in excess of 5 kHz and therefore, PLL phase noise should not be a major problem in maintaining correlation product's phase angle stability.

The degradation in angular stability for lower bandwidths is quite significant. A PLL with zero bandwidth acts as a free-running oscillator. This is where the RO is rejected entirely from the loop while at the same time passing the VCO only to the output as a free-running oscillator. Hence its behavior resembles the results obtained in [P4], which used a FRO for all its simulations. Otherwise, the standard deviation is inversely proportional to the loop bandwidth, which means that the deviations in phase angle over consecutive epochs can be reduced if the PLL loop bandwidth is increased. Increasing the frequency division ratio of the PLL worsens the overall phase angle stability for given values of VCO PN and PLL bandwidth. Nevertheless, it is still possible to easily maintain maximum phase deviations under 10 degrees for almost all the loop bandwidths typically used in commercial GNSS radio front-end PLLs.

5.5   *Results Analysis*

Table 5.2 and Table 5.3 describe the maximum PLL phase noise allowed at different combinations of loop bandwidth, frequency division ratio and integration time to maintain SNR above 50 dB and 30 dB respectively. To better interpret the values in Table 5.2, consider the case of bandwidth 30 kHz (shaded). For frequency division ratio N = 64, as the PIT is increased, the maximum phase noise allowed to maintain SNR above 50 dB also increases, or in other words, more phase noise is acceptable. If the frequency division

ratio is increased to 200, for the same PIT (e.g., 4 ms), to maintain SNR above 50 dB the phase noise requirement becomes more stringent (-112.5 dBc/Hz as compared to -105 dBc/Hz for FDR of N = 64). It can be observed that as we reduce the PLL loop bandwidth to 1 kHz, it starts to behave increasingly like a free running oscillator, and shows characteristics opposite to the higher BW cases. As an example, the SNR at a given PN reduces as the PIT is increased from 4 ms to 100 ms for bandwidth equal to 1 kHz. This conforms very well with the results obtained in [P4] and [P5], both of which used a FRO model as the frequency source.

5.6   *Endnote about Phase Noise and Allan Variance*

Oscillator manufacturers usually represent the performance of their products in terms of phase noise as a function of frequency difference from the center frequency, with units of dBc/Hz. Phase noise is a simple way to evaluate the performance of an oscillator as it is very easy to visualize on paper. However, it is debatable if this is indeed an informative metric for a GNSS receiver designer who may rather require a metric that will evaluate the oscillator performance in the time domain. Usually, the Allan Variance (AV) [112], [113], [114] is considered as a metric to provide such information, which is a derivative of the phase noise measurements over consecutive sample points. Would it be of interest to investigate the carrier and code tracking jitter as a function of oscillator AV as well, particularly:

- Is it possible to recreate this study using Allan Variance instead of Phase Noise?
- Is it possible to simulate overall Allan Variance of the PLL taking into account Allan Variance of each sub-block within the PLL?

In our opinion, AV and jitter measurements are computed using the phase noise power spectral density (PSD). It is possible that different PSDs can result in the same AV. Furthermore, the same AV (even though from different PSDs) may result in different bit error rate (BER). Hence, the PN PSD is more explicit measure that is nevertheless easily convertible to AV.

(a)

(b)

(c)
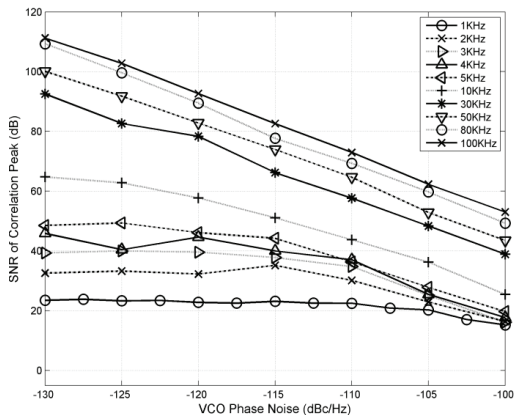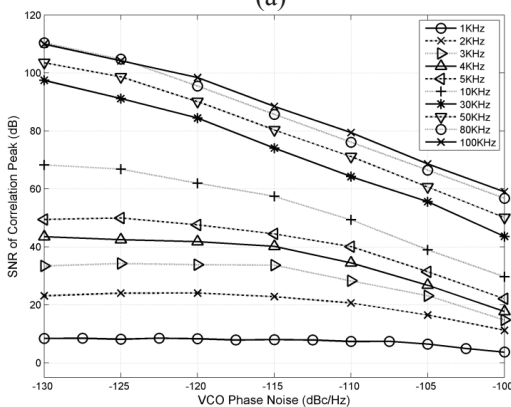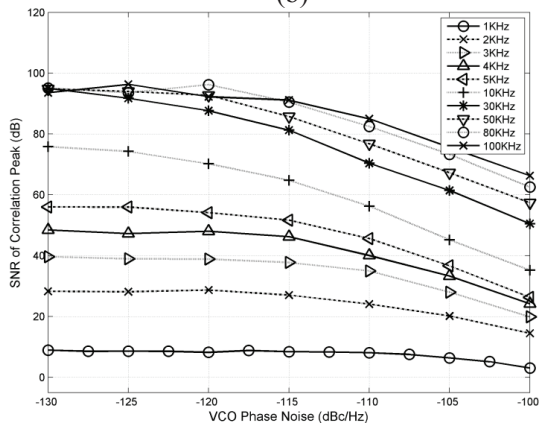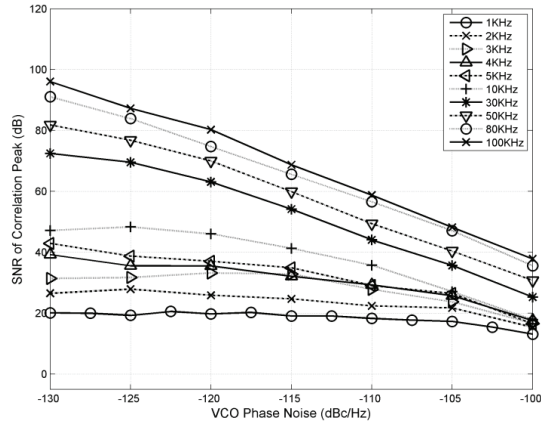
(d)
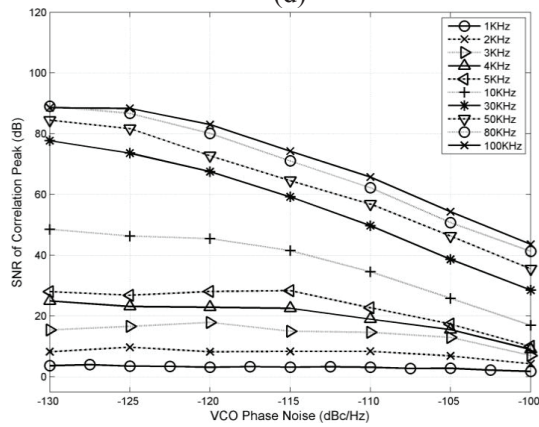
(e)
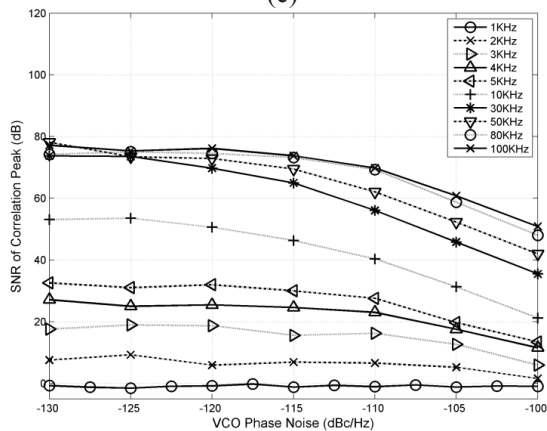
(f)

Fig. 5.5 Correlation SNR vs VCO PN with N = 64 and PIT = a) 4ms b) 20ms c) 100ms.
N = 200 and PIT = d) 4ms e) 20ms f) 100ms

(a)

(b)

(c)

(d)

(e)

(f)
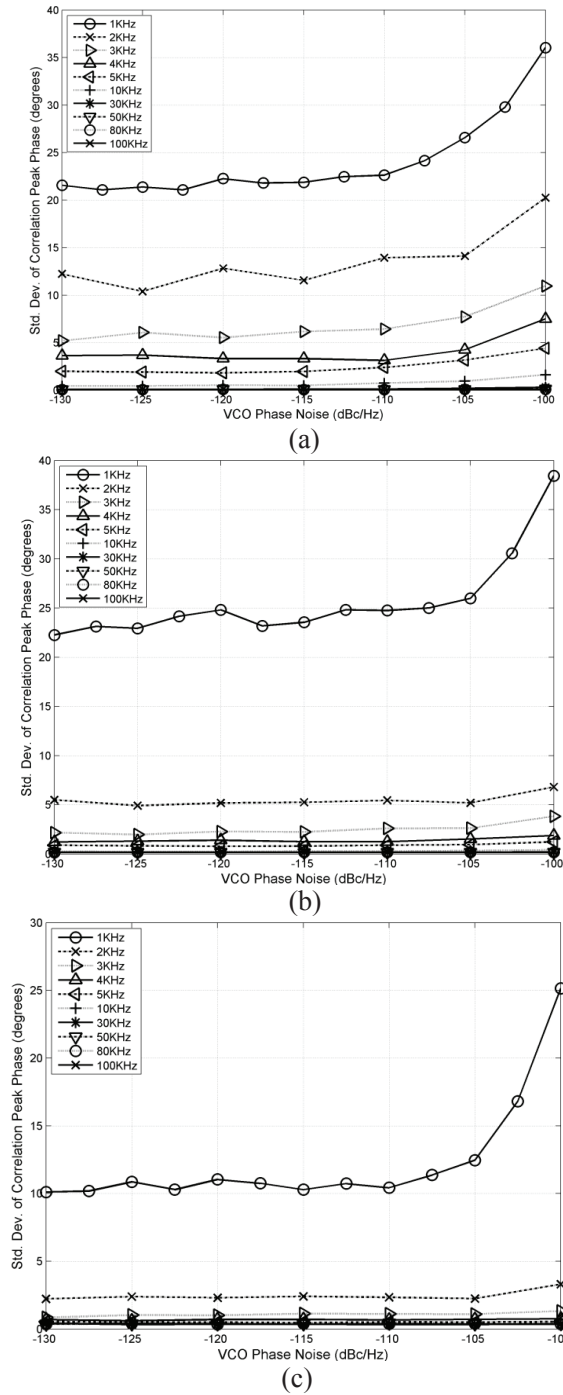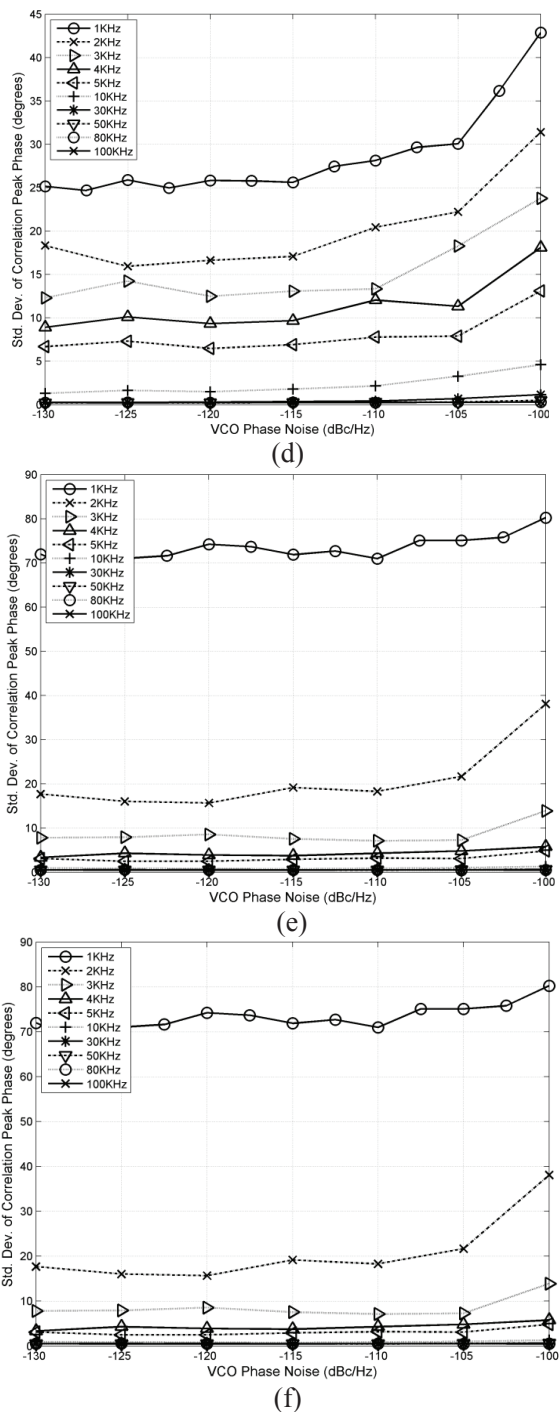
Fig. 5.6 Correlation Phase vs VCO PN with Freq Div = 64 and PIT = (a) 4ms (b) 20ms
(c) 100ms. Freq Div = 200 and PIT = (d) 4ms (e) 20ms (f) 100ms

Table 5.2 Maximum phase noise (dBc/Hz) in order to maintain minimum correlation SNR of 50 dB for different values of loop BW, PIT and frequency division ratio (N)

BW (kHz)	$N = 64$			$N = 200$		
	PIT = 4msec	PIT = 20msec	PIT = 100msec	PIT = 4msec	PIT = 20msec	PIT = 100msec
5	-125	-125	-113	-	-	-
10	-115	-110	-107	-	-	-119
30	-105	-102.5	-100	-112.5	-110	-107
50	-102.5	-100	> -100	-110	-107	-104
80	-100	> -100	> -100	-105	-105	-101
100	> -100	> -100	> -100	-105	-103	-100

Table 5.3 Maximum phase noise (dBc/Hz) in order to maintain minimum correlation SNR of 30 dB for different values of loop BW, PIT and frequency division ratio

BW (kHz)	FDR = 64			FDR = 200		
	PIT = 4msec	PIT = 20msec	PIT = 100msec	PIT = 4msec	PIT = 20msec	PIT = 100msec
1	-	-	-	-	-	-
2	-110	-	-	-	-	-
3	-107.5	-111	-106	-112	-	-
4	-107	-107	-103	-111	-	-
5	-106	-104	-102	-111	-	-115
10	-102	-100	> -100	-107	-107.5	-104.5
30	> -100	> -100	> -100	-102	-101	> -100
50	> -100	> -100	> -100	-100	> -100	> -100
80	> -100	> -100	> -100	> -100	> -100	> -100
100	> -100	> -100	> -100	> -100	> -100	> -100

6. TEST SCENARIOS FOR ADVANCED GNSS RECEIVERS

6.1   Introduction and Background

The objective of this section is to serve as a guideline for the testing and performance validation of GNSS receivers. We follow the typical testing procedure for GNSS receivers as shown in Fig. 6.1 and the test scenarios described in [17]-[26]. However, the aim is to adapt these scenarios, (which are targeted primarily towards simple receivers) to the more advanced multi-frequency, multi-constellation GPS L1/L5, Galileo E1/E5a TUTGNSS prototype receiver. Publication [P7] extends this discussion further by demonstrating how these test cases can be incorporated into an automated test-bench. Together, this information describes our work in investigating novel solutions for Block 3 from Fig. 1.1.

6.2   Receiver Settings

Two configuration settings in the receiver control the mode of operation and the manner in which it has to be turned ON via a 32-bit control word. Table 6.1 describes the various options and the digital control word corresponding to each option. There are eight possible modes of operations which would require 3 bits to be uniquely represented. However, it is recommended to use 5 bits in order to accommodate any future increase in operating modes. Similarly, there are three ways to turn ON a receiver, which can be uniquely represented by 2 bits. Therefore, out of the 32 available bits, only 7 bits are currently utilized, leaving the rest in reserve for future use. The mode selection bits are in the least significant bit (LSB) position of the control word. As an example, if the receiver should

perform position fix after a warm start using GPS L1 and Galileo E1 signals, the 32-bit control word would be "00000000_0000000_00000000_00100010". Using such a control word at the beginning of every test, it is possible to use the following scenarios to test a basic single constellation or more advanced multi-constellation receiver.

6.3 *Time to First Fix (TTFF) Tests*

The amount of time it takes the receiver after switching ON to compute the first valid position fix is called time-to-first-fix or TTFF. Depending upon the initial conditions, there are four start modes for a typical GNSS receiver: cold start, warm start and hot start [14]. In cold start, the receiver has no a-priori information about the on the approximate time, ephemeris, almanac or last computed position, and TTFF may take around 60 seconds under nominal signal power. In warm start conditions, the receiver has a-priori information about the approximate time, last computed position, oscillator offset and a valid copy of the almanac is stored in memory. The ephemeris is yet to be decoded and hence the time-of-week information is missing, resulting in a TTFF close to 30 seconds. In hot start conditions, the receiver has a-priori information about all data required for a position fix. Valid ephemeris and almanac are available for all visible satellites, along with approximate time, oscillator offset, and last position fix, resulting in a TTFF of about 1 second.

6.3.1 *Nominal Cold Start, Warm Start and Hot Start TTFF*

The aim of this test is to verify receiver's cold start, warm start and hot start TTFF performances under nominal signal conditions, typically assumed as satellite signal power equal to or greater than -130dBm.

6.3.2 *Low Power Cold Start TTFF*

The aim of this test is to verify the receiver's cold start TTFF performance under low power input signal conditions, typically assumed as maximum satellite signal power equal to or less than -142 dBm.

START

Define the Overall
Receiver System

Prepare the Receiver
Specifications and
Requirements

Prepare the Test-
Plan (Traceability
Matrix and Test
Cases)

Perform the Tests on
the Receiver

Analyze why the
Test Results are
Unsatisfactory.
Modify the
Receiver Hardware
and/or Software
Accordingly

Record Test Results

Are Test
Results
Satisfactory
?

No

Yes

END
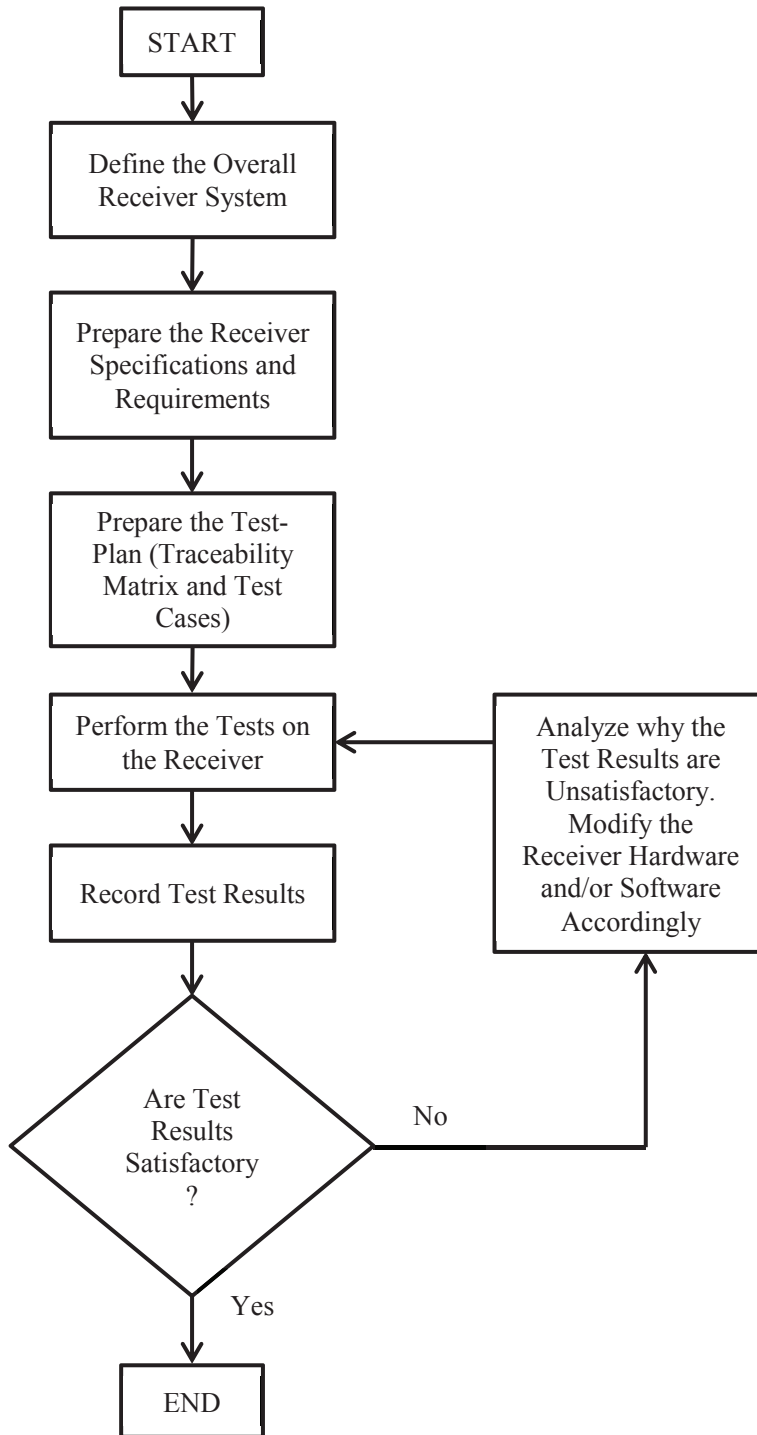
Fig. 6.1 Typical testing procedure for GNSS receivers

Table 6.1 Advanced GNSS receiver operating modes

	Example Options	Binary Representation
Example modes of operation	GPS L1 only	00000
	Galileo E1 only	00001
	GPS L1 + Galileo E1	00010
	GPS L1 + GPS L5	00011
	Galileo E1 + Galileo E5a	00100
	GPS L1 + GPS L5 + Galileo E1 + Galileo E5a	00101
	GPS L1 + GPS L5 + Galileo E1	00110
	GPS L1 + Galileo E1 + Galileo E5a	00111
Turn ON modes	Cold Start	00
	Warm Start	01
	Hot Start	10

6.4   *Acquisition Sensitivity in Cold Start*

The aim of this test is to verify the receiver's acquisition sensitivity. Acquisition sensitivity refers to the minimum satellite signal power level at which the receiver can still perform successful acquisition. To perform this test, one satellite in the simulator is maintained at a defined power level and required numbers of acquisition iterations are performed. In each iteration, acquisition is deemed successful only if the code delay and the Doppler offset estimated by the receiver acquisition is within ±1 chip (300m) and ±150Hz respectively from the correct (simulator) values. If the percentage of successful acquisitions is greater than a pre-determined threshold, the receiver is thought to acquire satellites successfully at this power level. The satellite signal power is then reduced and the test repeated.

6.5   Accuracy

Position accuracy is defined as the magnitude of the distance between the computed position of the receiver and the true position as defined in the simulator. 2-dimensional position accuracy is usually represented in terms of Circular Error Probability (CEP), while 3-dimension position accuracy is expressed in terms of Spherical Error Probability (SEP). CEP is the radius of a circle which encompasses half of the position fixes. Better the accuracy of the receiver, closer to the true position will be its repetitive position fixes, thus smaller will be the radius of the circle encompassing half of these points.

6.6   Tracking Sensitivity

Tracking sensitivity of a receiver is defined as the minimum satellite signal power at which the receiver can still continue tracking the satellite. To perform this test, the signal power of a visible satellite is switched between nominal and a low power level at regular intervals and over a number of iterations. The tracking performance, in terms of CNR of the satellite as measured by the receiver is continuously monitored over the power variations to ensure that it is indeed successfully tracking the satellite. In the next iteration, the low power level is reduced by 1 dB and the process is repeated. It is interesting to identify what benefits in tracking advanced receivers offer over single-frequency single-constellation receivers. Furthermore, when using GPS L5/Galileo E5a signals, it is necessary to specify whether this refers to only pilot signal tracking or to combined data and pilot signal tracking.

6.7   Availability

Availability refers to the percentage of time services of the GNSS receiver are useable. Differently put, it refers to the percentage of time valid position fix is computed by the receiver under diverse conditions of signal strength. Under this scenario, the receiver is subjected to diverse signal power, interference and multipath conditions, which attempt to recreate outdoor, urban canyon and indoor environments. Receiver motion is simulated by changing the simulator signal characteristics at regular intervals. Throughout the scenario, the receiver performance is monitored to ensure that it continues to provide a valid

position solution. The percentage of time that the receiver experiences an 'outage' is then used to compute the availability of the receiver.

6.8   Receiver Dynamics

This scenario is used to test the performance of the GNSS receiver when in motion. The important parameters of motion are speed, direction, acceleration, jerk and instantaneous position. Typically, receiver dynamics are tested for speeds up to 120 km/h. [18] proposes a circular trajectory, while [17] proposes a racetrack trajectory (also called a rectangular trajectory with rounded corners), as shown in Fig. 6.2. This figure also shows some example values for the top/bottom path distance = 1440m, left/right path distance = 940m, corner radius = 20m, position of starting point = left hand top corner, direction of rotation = clockwise, acceleration distance = 500m, minimum speed = 30 km/h on turn, and maximum speed = 120 km/h on straight path. Moving over the selected route three times allows a more general idea of receiver performance under dynamic stress. If the receiver is capable of mapping the route as it is in motion, this is convenient for post-processing of the positioning accuracy and availability during the dynamic scenario.

6.9   Reacquisition Time

Reacquisition time is defined as the time necessary for a receiver to reacquire all visible satellites and make a position fix after a sudden drop in signal power causes all previously tracked satellite signals to be lost. Quick reacquisition time is important, e.g., in vehicle navigation systems. To perform this scenario, the receiver is first allowed to make a stable position fix under nominal satellite signal power conditions. Next, all the visible satellite signals from the simulator are turned OFF until the receiver no longer is tracking any of them. Finally, all the signals are turned ON simultaneously at nominal power level. The amount of time it takes for the receiver to re-obtain stable position fix is measured as the reacquisition time.
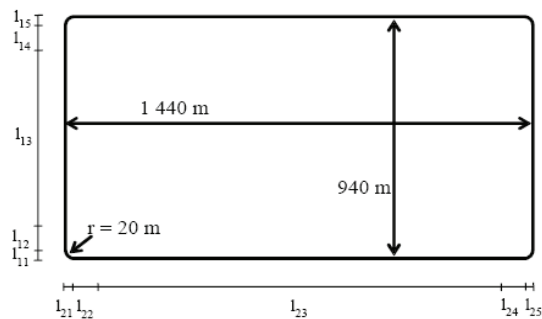
Fig. 6.2 Rectangular (racetrack) trajectory for dynamics testing

6.10   Multipath Mitigation

The objective of this test is to determine the ability of the receiver in mitigating the effect of multipath errors, including Non Line-Of-Sight (NLOS) multipath components. Signal simulators have inbuilt support for a number of realistic multipath scenarios and models, which can be used for performing this test. Multipath errors are a significant source of receiver performance degradation, considering that the number of satellite navigation receivers in smartphones/Personal Navigation Devices (PNDs) is continuously rising, and majority of such receivers are typically used in urban high-multipath conditions.

6.11   Radio Frequency Interference (RFI)

The objective of this test is to determine the ability of the receiver to operate in the presence of interfering signals, including non-intentional and intentional (jamming) interferers. The most convenient option is to check whether in presence of radio frequency interference of up to -60 dBm, the receiver continues to maintain stable position fix. Testing can be performed for interference mitigation on a single GNSS frequency band or on all frequency bands processed by the receiver.

6.12   Ionosphere errors

The objective of this test is to investigate the performance of the dual-frequency receiver approach in compensating for the ionosphere error and improving the accuracy of position

fix. This scenario can be performed by computing the receiver accuracy in single-frequency mode of operation, followed by the dual-frequency mode. The benefit of using dual-frequency can be quantified in terms of meters of improved accuracy. Signal simulators are capable of generating ionosphere errors based on one or more mathematical models, which can be used for performing this test. However, it should be noted that, using the same mathematical model to generate ionosphere errors in the simulator as that used for ionospheric error compensation within the receiver can result in an unrealistically improved performance of the receiver.

7. OVERVIEW OF PUBLICATIONS

7.1   *Research Problems and Proposed Solutions*

During the course of this thesis work, the research group was presented with a number of challenges emanating from the performance testing of the TUTGNSS receiver in the final stages of the GRAMMAR project. This necessitated the design of an overall test-plan and development of the individual test-cases for the important performance parameters. The solutions to these challenges were compiled and gradually evolved into the composition of this manuscript.

During the test-plan, it was noticed that the research group at TUT did not possess a GNSS signal source capable of producing the multiple frequencies and multiple constellations necessary for full performance evaluation of the advanced TUTGNSS receiver. Consequently, it was planned to investigate the possibility of developing a software-based signal simulator capable of generating the required signals. The first step towards this was a background study of important performance parameters of GNSS receivers and their typical test-scenarios. Also included in this study was a literature study of state-of-art in software-based GNSS simulators within the academic and industrial domains. Simultaneously, it was decided to investigate another novel solution for a GNSS signal source, which was to implement a radio front-end capable of receiving all possible GNSS signals from the sky using the concept of wideband sampling.

During the actual testing of the TUTGNSS receiver, it was observed that manual intervention was unsuitable for repetitive testing as it was inefficient and introduced errors into the test results. Moreover, without an internal view of the signal processing chain at every stage of the receiver, it was difficult to locate the cause of receiver performance

anomalies. Therefore, the next challenge was to design an automated test-bench that would remove the need for human control, and a data capture tool for accessing intermediate results from within the receiver processing chain.

The third and final challenge addressed by this thesis was to study the degrading effect of phase noise from the radio front-end's local frequency generator on the baseband tracking performance of the GNSS receiver. The objective of this study was to demonstrate that there exists possibility to design innovative test scenarios for GNSS receivers through the study of new performance metrics. The solution to this problem included designing mathematical models for simple free running oscillators and consequently, a more realistic PLL, in terms of their phase noise contributions, which were then used to study the performance of typical carrier and code tracking loops under diverse operating environments.

7.2   *Relating Publications to the Research Work*

The publications included in this manuscript are referred to as [P1] – [P7] in the following paragraphs. Fig. 1.1 and Table 1.1 describe how the individual Publications contribute to the overall research theme. Publications [P1], [P2] and [P3] describe the work done towards implementing novel sources of test signals for GNSS receivers. Two solutions are proposed for this problem: a software-based signal simulator with multi-frequency, multi-constellation capability, and a bandpass-sampling based sampled data generator. These publications build upon the introduction about general theory of software-based simulators and wide-band sampling provided in Chapters 3 and 4 respectively.

Chapter 5 presents a brief introduction and background to the concept of phase noise, and our proposed study on its effects on GNSS tracking performance. Further details of this study are presented in publications [P4], [P5] and [P6]. In [P4] and [P5], a simple free-running oscillator phase noise model is used as the noise source, and its effects on a GPS and Galileo code and carrier tracking channel are investigated in terms of the signal to noise ratio and phase component of the correlation product. In [P6], the study is extended to include the effect of a more realistic PLL PN model on a GPS code tracking channel.

As described earlier, these publications deal with investigating novel applications for the test-bench and identifying novel parameters to characterize receiver performance.

Chapter 6 describes the typical test cases and test scenarios for the performance evaluation of GNSS receivers. An attempt has been made to adapt these scenarios so that they can be applied to more advanced multi-frequency, multi-constellation receivers. Publication [P7] describes the tool that assists in the automated performance evaluation of the receiver based on scenarios introduced in Chapter 6. It also describes a data capture tool to capture the internal process parameters from within the TUTGNSS receiver hardware.

Together, these publications describe the novel solutions that we propose for improving the efficiency, accuracy and diversity of GNSS receiver performance evaluation, which is the main theme of this thesis work.

7.3   *Author's Contribution to the Publications*

The author has been the lead contributor to a majority of the publications included in this manuscript. However, as in any research activity, collaboration between internal and external research partners has been a significant driver for these publications. Here we attempt to specify the actual contribution of this author to each one of the listed publications [P1] – [P7].

In [P1], this author formulated the research problem based on the prevailing situation in the research group with regards to the testing of the TUTGNSS prototype receiver. This was followed with an in-depth literature review of the state-of-art software-based simulators, including categorizing them in three generations based on their year of creation, listing their constituent components, strengths and weaknesses, and identifying a pattern in the evolution of such simulators over the past 20 years. By extrapolating this pattern, a set of criteria for an advanced software-based simulator were proposed. A Simulink-based model was developed which attempted to incorporate some of the components of such advanced simulators. The co-authors assisted in the formulation of the research problem, suggested additional parameters on which the simulators could be compared and helped to review the publication manuscript.

In [P2] and [P3], this author prepared the design for the Sampled Data Generator in collaboration with research supervisors (who were also the co-authors) after a detailed literature review of multi-frequency GNSS receivers and the general theory of bandpass-sampling. The low noise amplifier design, simulations, and PCB-based implementation were accomplished by this researcher. Testing of the LNA was performed in collaboration with a supervisor from the RF Department. This was followed by Matlab-based simulations of the bandpass-sampling theorem to identify the most suitable sampling frequency for the proposed SDG. The composition of these publication manuscripts was accomplished by this author with peer-reviews provided by the co-authors.

In [P4], the original idea for the research direction was suggested by two of the co-authors, who also contributed to the theoretical formulation of the research problem. They performed the time-domain and frequency-domain analysis of the effect of free running oscillator phase noise on a typical GNSS code tracking loop. This author designed the Matlab-based simulations, performed experiments to verify that the effect of phase noise on code tracking was in conformance to the theoretical stipulations, recorded the results, and made conclusions from the analysis about the nature of the relationship between tracking performance and radio front-end phase noise. In [P5] the idea to extend the analysis from [P4] to carrier tracking loops was proposed by a co-author. This author extended the mathematical models for the code tracking loops to incorporate also carrier tracking (phase angle information of the correlation product) in a similar analysis using Matlab-based simulations.

In [P6], the publication was a result of equal collaboration between this author and the next significant co-author. The RF research group was involved in implementing a detailed mathematical model of a charge-pump PLL, including the phase noise contribution of its constituent blocks. This author was responsible for implementing the GNSS tracking and correlation model in Matlab and simulating the effect of the phase noise on the tracking loop performance, which resulted in detailed guidelines about radio front-end PLL circuit design for GNSS receivers. This study was more comprehensive than the previous studies using free running oscillator PN models. The analysis of the results provided for more practically useful metrics and thresholds for receiver designers.

In [P7], two major themes are addressed: automation of the overall receiver testing using a custom software tool called the AutoPET, and introducing the capability to characterize the signal processing chain using the data capture tool called dCAP. The AutoPET is a software program in the Qt platform and C++ language that communicates between the GNSS receiver, the test signal source and a control computer to achieve human-independent testing of the receiver. The entire assembly, including the communication between the entities was designed and implemented by this researcher. The data capture tool called dCAP, was implemented in hardware by the next significant co-author. The integration of these tools into the overall test-bench, and composing the publication was accomplished by this author.

7.4   Impact of Publications

There has been a conscious attempt by the author to propose the results of the thesis work for publication at high quality, high impact conferences and journals in accordance with the Finnish Publication Forum (Julkaisufoorumi – Jufo, for short) [111]. In case of publications in venues not listed in the forum, the author has chosen recommended conferences from the field of navigation and positioning. Additionally, Chapter 3 of this manuscript has been adapted as a book chapter in [116]. Below is a list of publications and their respective venues, supporting the earlier remarks:

[P6]   - Jufo Level 2 Journal

[P5] & [P3]   - Jufo Level 1 Conferences

[P1]   - European Navigation Conference (ENC-GNSS)

[P7]   - Institute of Navigation's GNSS+ Conference (ION GNSS+)

[P4]   - InsideGNSS

[P2]   - IEEE, ESA, and DLR Co-sponsored Conference

8. CONCLUSIONS

8.1   *Main Contributions of the Research*

The principle contributions of this research work are towards GNSS receiver performance evaluation through innovations in implementation of a test-bench, its automation techniques and application procedures. After an in-depth study of the state-of-art in GNSS software-based signal simulators, showing that such simulators have evolved through three distinct generations, a further study was conducted on multi-frequency, multi-system GNSS receiver performance testing and its necessary simulator architectures. Based on this study, a GNSS signal simulator in software capable of producing GPS L1 and Galileo E1 B/C signals was implemented.

Another contribution of this thesis is a bandpass-sampling based sampled data generator capable of processing multiple GNSS frequencies. Implementation of the constituent LNA is covered in detail. The design, simulation, implementation and test results prove that the LNA successfully satisfied requirements of wide bandwidth, high gain, high linearity, frequency stability and low noise figure and compares very well with the state-of-art in such amplifiers. The process for calculating the optimum sampling frequency and resultant intermediate frequencies for the bandpass-sampling ADC was automated for all possible input signal conditions. Both, real and complex sampling was addressed.

A third contribution of this research work is the automation in receiver testing through the implementation of the AutoPET and dCAP. These tools are portable (software platform-independent), easy to install and execute on any computer with the basic scientific software and enable highly efficient and accurate testing of GNSS receivers. From an academic point of view, the dCAP is useful for teaching the spectral characteristics of

GNSS signals at every stage from deep inside the receiver to researchers or university students in laboratory exercises. In other words, the proposed research has a practical as well as academic appeal.

As an application of the test bench, the effects of an FRO and a PLL phase noise on the tracking performance of a GNSS receiver were analyzed. A mathematical model for the PLL PN incorporating the PN contributions from its constituent sub-blocks was implemented and validated using Matlab and Simulink based GPS and Galileo correlators. The relation between integration time, PLL parameters and phase noise has been shown, and a criterion for radio front-end frequency generator design has been presented.

8.2   Future Work

In the duration of this research work, some ideas, concepts and implementation paths were left to be resolved in the future due to time and task prioritization. It is hoped that the receiver testing and the GNSS research community in general would be interested in following-up on the leads that this thesis has provided.

A number of challenges in the implementation of the sampled data generator have yet to be fully addressed. As an example, SNR degradation due to jitter, noise aliasing, quantization and high power consumption leading to ADC thermal issues have yet to be quantified and can be a subject of further research along with possible solutions to mitigate their effects. The PLL phase noise model in Matlab can be integrated with the software-based GNSS signal simulator as an additional source of receiver error. It can also be converted into a physical device using programmable hardware logic and VHDL coding. This physical PLL (P-PLL) can then be integrated with a VHDL-based GNSS signal simulator and their combined signals can be studied using the TUTGNSS prototype. With regards to the automated test-bench, there is a need for further study on the testing procedures employed for receivers used in more diverse applications of satellite-based positioning receivers, e.g., military, indoor navigation and high-accuracy positioning. These test cases can be added to the library of the AutoPET and dCAP tools, thus expanding their application areas.

BIBLIOGRAPHY

[1]   T. Paakki, J. Raasakka, F. Della Rosa, H. Hurskainen, J. Nurmi, TUTGNSS University based hardware/software GNSS receiver for research purposes, Proceedings of the 2010 Ubiquitous Positioning Indoor Navigation and Location Based Service (UPINLBS 2010), vol. 1, no. 6, pp. 14-15, Oct. 2010.

[2]   U. Weinbach, S. Schön, "GNSS receiver clock modeling when using high-precision oscillators and its impact on PPP", Journal on Advances in Space Research, January 2011, Volume 47 Issue 2, pp 229-238.

[3]   D. W. Allan, "Statistics of Atomic Frequency Standard", Proceedings of the IEEE, Vol 54, No. 2, Feb 1966, pp. 221–230.

[4]   W. Stockwell, "Bias Stability Measurement: Allan Variance", Crossbow Technology Inc. Available at: http://www.xbow.com/pdf/Bias_Stability_Measurement.pdf.

[5]   NASA Goddard Space Flight Center, "GNSS Data Sets", Crustal Dynamics Data Information System (CDDIS). Available at: http://cddis.nasa.gov/gnss_datasum.html.

[6]   "EU-U.S. Cooperation on Satellite Navigation", Working Group C, ARAIM Technical Subgroup, Interim Report, Issue 1.0, December 19th, 2012.

[7]   Federal Aviation Administration, "Phase II of the GNSS Evolutionary Architecture Study", February 2010. Available at: http://www.faa.gov/about/office_org/headquarters_offices/ato/service_units/techops/navservices/gnss/library/documents/media/GEASPhaseII_Final.pdf

[8]   A. M. A. Farah, "GPS/Galileo simulation for reduced dynamic LEO satellite orbit determination", University of Nottingham PhD Thesis 2004, UK.

[9]   Jet Propulsion Laboratory, California Institute of Technology, "Global Ionospheric (TEC) Maps". Available at: http://www.gdgps.net/products/tec-maps.html.

[10] Magellan Professional, "Manually Downloading US National Geodetic Survey CORS data", January 2007. Available at: ftp://ftp.ashtech.com/Mobile%20Mapping/MobileMapper%20Office%20for%20M MCX%20&%20MMPro/Application%20Notes/Manually%20downloading%20US %20NGS%20CORS%20data.pdf.

[11] Y. Memarzadeh, "Ionospheric Modeling for Precise GNSS Applications", Delft University of Technology Ph.D. Thesis, the Netherlands, December 2009. Available at: http://www.ncg.knaw.nl/Publicaties/Geodesy/pdf/71Memarzadeh.pdf.

[12] A. Dolgansky, A. Szeto and S. Bisnath "Software Simulation Of Multiple Global Navigation Satellite System Measurements", Proceedings of the IEEE Toronto International Conference – Science and Technology for Humanity 2009 (TIC-STH 2009), September 2009, Toronto, Canada.

[13] S. Pullen, J. Rife, "Differential GNSS: Accuracy and Integrity", from the book GNSS Applications and Methods, (Eds.) S. Gleason, D. Gebre-Egziabher, Artech House, 2009, ISBN-13: 978-1-59693-329-3.

[14] F. van Diggelen, "A-GPS: Assisted GPS, GNSS, and SBAS", Edition 1, March 2009, ISBN- 10: 1596933747, ISBN-13: 978-1596933743.

[15] Fernández, J. Diez, A. Caramagno, "GRANADA-Galileo Receiver Analysis and Design Application", ESA-GJU Workshop on Tools and Facilities for Galileo Receivers, March 2006.

[16] B. Shen, Q. Zhang, "A New Method for Analyzing the Quantization Effect of ADC in Broadband QAM Receiver", Proceedings of the 2002 IEEE International

Conference on Communications, Circuits and Systems and West Sino Expositions, June 2002, pp 1262-1266.

[17] 3rd Generation Partnership Project (3GPP); 'TS34.171'; Technical Specification, V6.5.0 (2006-10).

[18] A. Mitelman, P. Nomark, M. Reidevall, S. Strickland, "Apples to Apples - Standardized Testing for High-Sensitivity Receivers", GPS World, January 1, 2008.

[19] Spirent Communications, "Testing GNSS System Errors", Application Note: DAN002, Issue 1-01.

[20] Spirent Communications, "Fundamental GNSS Receiver Characterisation", Application Note DAN003, Issue 1-01.

[21] Agilent Technologies, "Typical GPS Receiver Verification Tests Using a GPS Signal Simulator", Application Note, May 2008.

[25] Spirent Communications, "Simulation versus Real World Testing - How to undertake controlled testing of your GNSS receiver design". Available at: http://www.insidegnss.com/special/elib/Spirent_Simulation_vs_Real_World_Testin g.pdf.

[26] National Instruments, "The Case for GPS Simulation". Available at: http://www.insidegnss.com/special/elib/NI_GPS_Simulation.pdf.

[27] Alliance for Telecommunications Industry Solutions, ATIS Telecom Glossary 2007 (Updated version of Federal Standard 1037C). Available at: http://www.atis.org/glossary/.

[28] T. H. Hee, A. Hajimiri, "Oscillator Phase Noise: A Tutorial" IEEE Journal on Solid-State Circuits, March 2000, vol. 35, no. 3, pp. 326-336.

[29] P. Misra, P. Enge, "Global Positioning System: Signals, Measurements, and Performance", Second Edition, 2006, ISBN: 0-9709544-1-7.

[30] B. Parkinson, J. Spilker (Editors), "Global Positioning System: Theory and Applications", Volume 1, ISBN: 1-56347-106-X.

[31]   E. Kaplan, C. Hegarty (Editors), "Understanding GPS: Principles and Applications", Second Edition, ISBN-10: 1-58053-894-0.

[32]   R. Giffard, "Estimation of GPS Ionospheric Delay Using L1 Code and Carrier Phase Observables", Proceedings of the 31st Annual Precise Time and Time Interval (PTTI) Planning Meeting, 7-9 December 1999, Dana Point, CA.

[33]   Kowoma.de, "The GPS System: Sources of Errors in GPS", November 2013. Available at: http://www.kowoma.de/en/gps/errors.htm.

[34]   Navstar GPS, "Navstar GPS User Equipment Introduction", September 1996. Available at: http://www.navcen.uscg.gov/pubs/gps/gpsuser/gpsuser.pdf.

[35]   J. Mendizabal S. J. M. Lagunilla, R. B. Perez, "GPS and Galileo: Dual RF Front-end Receiver and Design, Fabrication, and Test", McGraw Hill 2009, ISBN 978-0-07-159869-9.

[36]   Aerospace Corporation, "How GPS Works, GPS Primer". Available at: http://www.aero.org/education/primers/gps/howgpsworks.html

[37]   R. B. Langley, "Why is the GPS signal so complex?", GPS World, May/June 1990.

[38]   Navstar GPS, "Global Positioning System Standard Positioning Service Signal Specification", Second Edition, 2nd June, 1995.

[39]   Navstar GPS, "Global Positioning System Interface Control Document, IS-GPS-200G", 5th September, 2012.

[40]   European Commission, "Galileo Open Service, Signal in Space Interface Control Document, (OS SIS ICD)", Draft 1.1, September 2010.

[41]   "Global Navigation Satellite System (GLONASS), Interface Control Document", Edition 5.1, Coordination Scientific Information Center, Moscow, 2008.

[42]   China Satellite Navigation Office, "BeiDou Navigation Satellite System, Signal in Space Interface Control Document, Open Service Signal B1I", Version 1.0, December 2012.

[43]   S. Wallner, European Space Agency (ESA), Navipedia, "GNSS Signal", November, 2013. Available at: http://www.navipedia.net/index.php/GNSS_signal.

[44]   H. Hurskainen, T. Paakki, Z. Liu, J. Raasakka, J. Nurmi, "GNSS Receiver Reference Design", in Proceedings of 4th Advanced Satellite Mobile Systems (ASMS) conference 2008, Aug 26-28, 2008, Bologna, Italy, Pages: 204-209.

[45]   ESA Navipedia, "Tracking Loops", Available at: http://www.navipedia.net/index.php/Tracking_Loops.

[46]   V. G Dikshit, "Development of Global Navigation Satellite System (GNSS) Receiver", DRDO-IISc. Program on Mathematical Engineering Workshop, Bangalore, September 2007. Available at: http://pal.ece.iisc.ernet.in/PAM/work07.html.

[47]   M. S. Braasch, A. J. Van Dierendonck, "GPS Receiver Architectures And Measurements", Invited paper, Proceedings of the IEEE, Vol. 87, No. 1, January 1999.

[48]   M. Cummings, T. Cooklev, "Software Defined Radio (SDR) Technologies", Tutorial, International Symposium on System-On-Chip (SoC 2008), Tampere, 2008.

[49]   SDR Forum, "What is Software Defined Radio?". Available at: http://www.sdrforum.org/pages/aboutSdrTech/SoftwareDefinedRadio.pdf

[50]   V. Dvorkin, J. Wong, M. Zou, "Quad Demodulators Arm Direct-Conversion Receivers", Microwaves and RF, Feb 2004. Available at: http://mwrf.com/Articles/ArticleID/7470/7470.html

[51]   U. Mavric, "Digitizer Provides Direct Sampling Of RF Signals: Employing a simple RF signal chain, many potential limiting factors can be eliminated when directly sampling RF signals with high-speed analog-to-digital converters (ADCs)", Microwaves and RF, April 2006. Available at: http://mwrf.com/systems/digitizer-provides-direct-sampling-rf-signals

[52]   Trimble, Datasheet for Zephyr and Zephyr Geodetic GNSS antennas, 2007. Available at: http://www.navtechgps.com/assets/1/7/Zephyr_DS.pdf

[53]   Roke Manor Research/Siemens, Datasheet for Triple GNSS Geodetic-grade Antenna, 2006. Available at: http://www.roke.co.uk/resources/datasheets/042-gnss-antenna.pdf

[54]   J. Wang, D. Triplett (Wang Electro-Opto Corporation), "High-Performance Universal GNSS Antenna Based on SMM Antenna Technology", Proceedings of the IEEE 2007 International Symposium on Microwave Antenna Propagation and EMC Technologies for Wireless Communications, August 2007.

[55]   H. T. Friis, "Noise figures of radio receivers", Proceedings of I.R.E, July 1944.

[56]   L. E. Larson, "RF and Microwave Circuit Design for Wireless Communications", Artech House 1996, ISBN 0890068186.

[57]   C. Chien, "Digital Radio Systems on a Chip - A Systems Approach", First Edition, Springer 2001, ISBN 0792372603.

[58]   Jie-Cherng Liu, "Bandpass Sampling of Multiple Single Sideband RF Signals", Proceedings of the 2008 International Symposium on Communications, Control, and Signal Processing (ISCCSP 2008), Malta, 12-14 March 2008.

[59]   Ching-Hsiang Tseng, Sun-Chung Chou, "Direct Downconversion of Multiband RF Signals Using Bandpass Sampling", IEEE Transactions on Wireless Communications, Vol. 5, No. 1, January 2006.

[60]   Yi-Ran Sun, "Generalized Bandpass Sampling Receivers for Software Defined Radio", PhD Thesis, Royal Institute of Technology, Stockholm 2006.

[61]   M. L. Psiaki, D. M. Akos, J. Thor, "A Comparison of "Direct RF Sampling and Down-Convert & Sampling GNSS Receiver Architectures", Proceedings of the 2003 ION GPS/GNSS, 9-12 September 2003, USA.

[62]   D. M. Akos, M. Stockmaster, J. B. Y. Tsui, J. Caschera, "Direct Bandpass Sampling of Multiple Distinct RF Signals", IEEE Transactions on Communications, Vol. 47, No. 7, July 1999.

[63]   R. G. Vaughan, N. L. Scott, D. R. White, "The Theory of Bandpass Sampling", IEEE Transactions on Signal Processing. Vol. 39, No. 9. September 1991.

[64]   M. Psiaki, S. Powell, H. Jung, P. Kintner, "Design and Practical Implementation of Multifrequency RF Front Ends Using Direct RF Sampling", IEEE Transactions on Microwave Theory & Techniques, Vol. 53, No. 10, October 2005.

[65]   A. Latiri, L. Joet, P. Desgreys, P. Loumeau, "A Reconfigurable RF Sampling Receiver For Multistandard Applications", Académie Des Sciences, 2006.

[66]   N. Wong, Tung-Sang Ng, "An Efficient Algorithm for Downconverting Multiple Bandpass Signals Using Bandpass Sampling", Proceedings of the IEEE International Conference on Communications (ICC), June 2001, Helsinki, Finland.

[67]   M. Renfors, "Sampling and Multirate Techniques for Complex and Bandpass Signals", Lecture notes, Receiver architectures and signal processing, Tampere University of Technology.

[68]   T. J. Rouphael, "RF and Digital Signal Processing for Software-Defined Radio - A Multi-standard multi-mode approach", Elsevier Inc. 2009, ISBN 978-0-7506-8210-7.

[69]   N. Gray, "ABCs of ADCs – Analog to Digital converter Basics", National Semiconductor, June 2006. Available at: http://www.national.com/appinfo/adc/files/ABCs_of_ADCs.pdf

[70]   Invocom, Complex Signals and Sampling, Sampling and Multirate Processing of Bandpass and Complex (I/Q) Signals (Lesson 1), Invocom Tutorials, TUT. Available at: bruce.cs.tut.fi/invocom/p3-2/p3-2_3_1.htm

[71]   National Instruments, "Rational Resampling (Digital Filter Design Toolkit)", LabVIEW 8.6, Digital Filter Design Toolkit Help. Available at: http://zone.ni.com/reference/en-XX/help/371988B-01/lvdfdtconcepts/rational_resampling/

[72]   P. M. Corbell, M. M. Miller, "Design and Analysis of a Matlab Based Digitized IF GPS Signal Simulator and a Simulink Based Configurable GPS Receiver", Proceedings of ION GPS 2000, 19-22 September 2000, Salt Lake City, UT.

[73]   M. M. Miller, P. M. Corbell, J. F. Raquet, "Design and Validation of Digitized Intermediate Frequency GPS Signal and Receiver Software Models for Developing and Comparing Advanced GPS Receiver Technologies", Proceedings of ION GPS 2000, 19-22 September 2000, Salt Lake City, UT.

[74]   A. Brown, N. Gerein, K. Taylor, "Modeling and Simulation of GPS Using Software Signal Generation and Digital signal Reconstruction", Proceedings of the ION National Technical Meeting, January 2000, Anaheim, CA.

[75]   A. Brown and N. Gerein, "Advanced GPS Hybrid Simulator Architecture", Proceedings of ION 57th Annual Meeting, Albuquerque, NM, June 2001.

[76]   P. M. Corbell, M. M. Miller, "A Configurable GPS Accumulated I and Q Signal Component Simulator in Matlab", Proceeding of ION NTM 2001, 22-24 January 2001, Long Beach, CA.

[77]   T. H. Tan, "Global Positioning System Signal Simulation", Bachelor of Electrical Engineering (Honours) Thesis, The University of Queensland, Australia, October 2003.

[78]   L. Dong, "IF GPS Signal Simulator Development and Verification", Master of Science Thesis, University of Calgary, Canada, November 2003.

[79]   A. Nunes, T. Ferreira, J. Borràs, F. Nunes, F. Sousa, G. Seco, "Signal Generator and Receiver Toolbox for Galileo/GPS Signals", Proceedings of 2nd ESA Workshop on Satellite Navigation, Navitech 2004.

[80]   O. Julien, B. Zheng, L. Dong, G. Lachapelle, "A Complete Software-Based IF GNSS Signal Generator for Software Receiver Development", Proceedings of ION GNSS 2004, Sept. 21-24, Long Beach, CA.

[81] L. Dong, C. Ma, G. Lachapelle, "Implementation and Verification of a Software-Based IF GPS Signal Simulator", Proceedings of National Technical Meeting, Institute of Navigation, 26-28 January 2004, San Diego.

[82] C. Seynat, A. Kealy, K. Zhang, "A Performance Analysis of Future Global Navigation Satellite Systems", Journal of Global Positioning Systems (2004) Vol. 3, No. 1-2: 232-241.

[83] W. Kester, "Converting Oscillator Phase Noise to Time Jitter", Digi-Key Corporation, Techzone. Available at: http://www.digikey.com/us/en/techzone/wireless/resources/articles/converting-oscillator-phase-noise-to-time-jitter.html

[84] A. Pósfay, T. Pany, B. Eissfeller, "First Results of a GNSS Signal Generator Using a PC and a Digital-to-Analog Converter", Proceedings of ION GNSS 18th International Technical Meeting of the Satellite Division, 13-16 September 2005, Long Beach, CA.

[85] T. Inzerilli, D. Lo Forti, V. Suraci, "Modeling and Simulation of GNSS with NS2", Proceedings of 14th IST Mobile and Wireless Communications Summit, Dresden, June 2005.

[86] Accord Software & Systems Pvt. Ltd, "GPSLAB". Available at: http://www.gpslab.us/datasheet/DataSheet-prof.pdf

[87] A. Constantinescu, R.Jr. Landry, I. Ilie, "Hybrid GPS/Galileo/GLONASS IF Software Signal Generator", Proceedings of ION GNSS 18th International Technical Meeting of the Satellite Division, 13-16 September 2005, Long Beach, CA.

[88] NAVSYS Corporation, "GPS Signal Simulation Toolbox". Available at: http://www.navsys.com/brochures/NAVSYS_Toolbox.pdf

[89] C. Abart, P. Berglez, G. Abwerzger, B. Hoffmann-Wellenhof, W. Cresens, T. Vandeplas, W. De Win, "Simulating GNSS Constellations - The GAMMA Signal

Generator", Proceedings of the 20th International Technical Meeting of the Satellite Division of The Institute of Navigation (ION GNSS 2007), Fort Worth, TX.

[90]   Intecs,   "gLAB   GNSS   Signal   Analysis   Tool".   Available   at: http://www.intecs.it/pdf/brochure_gLAB_01-02-2010.pdf

[91]   VEGA IT GmbH, "Galileo System Simulation Facility (GSSF)". Available at: http://www.gssf.eu/Documents/GSSF%20V2.1%20Fact%20Sheet%20-%20Issue%201.pdf

[92]   K. Borre,"The E1 Galileo Signal", Lecture at Stanford University. Available at: http://waas.stanford.edu/~wwu/papers/gps/PDF/Borre/galileo_sig.pdf

[93]   C. Hu, M. Tsai, "The Implementation of an INS-GNSS Software Simulator", Proceedings of 28th Asian conference on Remote Sensing (ACRS 2007), November 2007, Kuala Lumpur, Malaysia.

[94]   I. Joo, J. Lee, S. Lee, J. Kim, D. Lim, S. J. Lee, "S/W based IF Signal Simulator Prototyping for L1 C/A, L2C, and E1(B/C)", Proceedings of The 9th International Conference on Information and Communications Security (ICICS 2007), December 2007, Zhengzhou, China.

[95]   C. Cosenza, Q. Morante, S. Corvo, F. Gottifredi, "GNSS Bit-True Signal Simulator-A Test Bed for Receivers and Applications", Satellite Communications and Navigation Systems, Signals and Communication Technology, 2008, 3, 447-460, DOI: 10.1007/978-0-387-47524-0_34.

[96]   F. Schubert, R. Prieto-Cerdeira, A. Steingass, "GNSS Software Simulation System for Realistic High-Multipath Environments", Proceedings of 4th ESA Workshop on Satellite Navigation User Equipment Technologies (NAVITEC 2008), December 2008, Noordwijk, The Netherlands.

[97]   J. Lee, T. Kim, S. Lee, J. Kim, "Development of Software GNSS Signal Generator", Proceedings of International Symposium on GPS/GNSS 2008, November 2008, Tokyo, Japan.

[98] S. Lim, D. Lim, M. Liu, S. W. Moon, C. Park, S. J. Lee, "Design of a Software-based Multi-Channel GNSS IF Signal Generator", Proceedings of International Conference on Control, Automation and Systems 2008, October 2008 in Seoul, Korea.

[99] German Aerospace Center (DLR), "Simulation of Satellite Navigation Signals and Channels (SNACKS)". Available at: http://snacs.sourceforge.net/index.html

[100] Fraunhofer Institute for Integrated Circuits IIS, "GNSS-SIGNAL-SIMULATOR". Available at: http://www.iis.fraunhofer.de/fhg/Images/07_GNSS-Signal_Simulator_neu_tcm278-158408.pdf

[101] TeleConsult Austria GmbH, "GNSS Multisystem Performance Simulation Environment (GIPSIE)". Available at: http://www.teleconsult-austria.at/download_public/GIPSIE.pdf

[102] Center for Remote Sensing Inc., "Software GNSS Signal Simulator". Available at: http://www.cfrsi.com/pdf/Software%20GNSS%20Signal%20Simulator.pdf

[103] Z. Y. Kou, Y. Huang, Z. Z. Qishan, "Architecture of software-based GNSS signal simulator and implementation of its IF signals generation", Journal of Beijing University of Aeronautics and Astronautics (2009-07), Available: http://en.cnki.com.cn/Article_en/CJFDTOTAL-BJHK200907004.htm

[104] C. Ouzeau, J. Korsakissok, "Performance Assessment of a Juzzle-Based GNSS Simulator", Proceedings of ENC GNSS 2009, May 2009, Naples, Italy.

[105] A. M. Smith, "Global Navigation Satellite System Signal Simulator - An Analysis of the Effects of the Local Environment and Atmosphere on Receiver Positioning", Doctor of Philosophy Thesis, University of Bath, UK, October 2007.

[106] University FAF Munich, "GNSS Software Simulation". Available at: http://www.ifen.unibw.de/research/gnss_simulator.htm

[107] Fernández, J. Diez, A. Caramagno, "GRANADA-Galileo Receiver Analysis and Design Application", ESA-GJU Workshop on Tools and Facilities for Galileo Receivers, March 2006.

[108] A. Dolgansky, A. Szeto and S. Bisnath "Software Simulation Of Multiple Global Navigation Satellite System Measurements", proceedings of the IEEE Toronto International Conference – Science and Technology for Humanity 2009 (TIC-STH 2009) in Toronto Canada.

[109] L. Marradi, G. Franzoni et. al, "The GARDA Project – Building a Galileo Receiver", InsideGNSS, November/December 2006, pp 40-53

[110] D. Boschen, "GPS C/A Code Generator", Matlab Central, Jun 2010. Available at: http://www.mathworks.com/matlabcentral/fileexchange/14670-gps-ca-code-generator&watching=14670.

[111] Finland Publication Forum, Julkaisufoorumi. Available at: http://www.tsv.fi/julkaisufoorumi/

[112] P. C. Chang, H. M. Peng, S. Y. Lin, "Allan Variance Estimated by Phase Noise Measurements", 36th Annual Precise Time and Time Interval (PTTI) Systems and Applications Meeting, Washington DC on 7-9 Dec 2004.

[113] Wenzel Associates, Inc., "Spreadsheets/Programs", Available at: http://www.wenzel.com/documents/spread.htm

[114] F. Ramian, "Time Domain Oscillator Stability Measurement Allan Variance", Application Note, Rhode&Schwarz, Feb 2012.

[115] R. El Assir, "Global Navigation Satellite Systems and Their Applications", Microwave Journal, Vol. 55, No. 5, pp. 142-152, May 14, 2012.

[116] J. Nurmi, S. Lohan, S. Sand, H. Hurskainen, (Eds.), "GALILEO Positioning Technology", Signals and Communication Technology Series, Vol. 182, ISBN 978-94-007-1829-6.

[117] V. Syrjala, M. Valkama, M. Renfors, "Design considerations for direct RF sampling receiver in GNSS environment", proceedings of the 5th Workshop on Positioning, Navigation and Communication, 2008 (WPNC 2008), March 2008, Hannover Germany.